수의학박사학위논문

피부세포와 3 차원 피부 모사체를 이용한 mannosylerythritol lipids 의 미백과 보습효과에 관한 연구

Whitening and moisturization efficacy of mannosylerythritol lipids in three-dimensional human skin equivalent and human skin cells

2019 년 2 월

서울대학교 대학원

수의학과 수의병리학 전공

배 일 홍

피부세포와 3 차원 피부 모사체를 이용한 mannosylerythritol lipids 의 미백과 보습효과에 관한 연구

Whitening and moisturization efficacy of mannosylerythritol lipids in three-dimensional human skin equivalent and human skin cells

지도교수 김 대 용 (D.V.M., Ph.D.)

이 논문을 수의학박사 학위논문으로 제출함
2018년 10월

서울대학교 대학원

수의학과 수의병리학 전공

배 일 홍

배일홍의 수의학박사 학위논문을 인준함
2018년 12월

위 원 장 _____ (인)

부 위 원 장 _____ (인)

위 원 _____ (인)

위 원 _____ (인)

위 원 _____ (인)

ABSTRACT

Whitening and moisturization efficacy of mannosylerythritol lipids in three-dimensional human skin equivalent and human skin cells

(Supervisor: Dae-Yong Kim, D.V.M., Ph.D.)

Il-Hong Bae

Department of Veterinary Pathology, College of Veterinary Medicine, Graduate School, Seoul National University

Mannosylerythritol lipids (MELs) are a type of extracellular glycolipids that are mostly produced by the yeast strains of genus *Pseudozyma*. MELs have been reported to have a few biochemical properties besides their original use as biocompatible biosurfactants to date. As the possible applications of MELs expand, many attempts are being made to find out yet-unknown biological potentials of MELs. In the present study, I demonstrated the yet-unreported biological efficacies of MELs

composed of 85% di-acylated MEL-B and 15% tri-acylated MEL and their underlying mechanisms associated with skin whitening and moisturizing using in vitro human skin cells and a three-dimensional human skin equivalent. In MELs' skin whitening efficacy experiment, MELs significantly decreased melanin contents both in normal primary human melanocytes (NHMs) and α-melanocyte-stimulating hormone-stimulated B16 murine melanoma cells. MELs treatment exhibited whitening effect in a human skin equivalent containing melanocytes, lightening the color and reducing the melanin content in the epidermis. Histologic analysis using Fontana Masson staining showed significant reduction of melanin content in the melanocytes. The autofluorescence signal intensity of melanin detected using two-photon excitation microscopy was significantly less in MELs-treated skin equivalents than in controls. The molecular mechanism underlying the anti-melanogenic effect induced by MELs treatment was associated with the inhibition of the ERK/CREB/MITF signaling pathway, which suppressed gene expression levels of key melanogenic enzymes including tyrosinase, tyrosinase-related protein-1, and tyrosinase-related protein-2 in NHMs. In the subsequent skin moisturizing efficacy experiment of MELs, I demonstrated that aquaporin-3 (AQP3) expression markedly reduced by UVA irradiation was alleviated by MELs treatment at both the protein and mRNA levels in culture human keratinocytes (HaCaT cells). MAPK inhibitor assay revealed that phosphorylation of JNK mediates UVA-

induced downregulation of AQP3, and that MELs treatment significantly inhibits UVA-induced phosphorylation of JNK. I additionally confirmed MELs suppressed the UVA-induced phosphorylation of JNK. I also found that PPAR-γ mRNA expression was downregulated in UVA-irradiated HaCaT cells, which was markedly counteracted by treatment with a JNK inhibitor or MELs. These findings suggest that MELs ameliorate UVA-induced AQP3 downregulation in HaCaT cells by suppressing JNK activation to block the decrease of PPAR-γ. Taken together, the present data herein demonstrate for the first time the new efficacy of MELs to exert a whitening effect by inhibiting melanogenesis in melanocytes and to mitigate UVA-induced AQP3 downregulation in keratinocytes. In addition, my findings support the potential development of MELs for pharmaceutical and/or cosmeceutical ingredient in human skin.

Keywords: mannosylerythritol lipids, melanogenesis, tyrosinase, human skin equivalent, aquaporin-3 (AQP3), ultraviolet A (UVA), c-Jun N-terminal kinase (JNK)

Student Number: 2013-30493

CONTENTS

ABBREVIATIONS

MELs: mannosylerythritol lipids

NHM: normal human melanocyte

α-MSH: α-melanocyte stimulating hormone

Tyrp-1: tyrosinase-related protein-1

Tyrp-2: tyrosinase-related protein-2

L-DOPA: L-3,4-dihydroxyphenylalanine

DHICA: 5,6-dihydroxyindole-2-carboxylic acid

MITF: microphthalmia-associated transcription factor

POMC: proopiomelanocortin

PKA: protein kinase A

cAMP: adenosine 3',5'-monophosphate

CREB: cAMP-responsive element binding

MAPK: mitogen-activated protein kinase

MEK: mitogen-activated protein kinase kinase

ERK: extracellular signal-regulated kinase

RSK: ribosomal s6 kinase

AQP3: aquaporin-3

SC: stratum corneum

TEWL: transepidermal water loss

UVR: ultraviolet radiation

UVA: ultraviolet A

UVB: ultraviolet B

PPAR−γ : peroxidase proliferator activated receptor−γ

JNK: c−Jun N−terminal kinase

qRT−PCR: quantitative real−time polymerase chain reactions

GAPDH: glyceraldehyde−3−phosphate dehydrogenase

RPLP0: ribosomal protein lateral stalk subunit P0

FBS: fetal bovine serum

SDS: sodium dodecyl sulfate

PAGE: polyacrylamide gel electrophoresis

TBST: tris−buffered saline containing Tween−20

H&E: hematoxylin and eosin

F&M: Fontana−Masson

TPEF: two−photon excitation fluorescence

LITERATURE REVIEW

Introduction

Mannosylerythritol lipids (MELs) are functional glycolipids, which composed of 4−O−β−D−mannopyranosyl−erythritol or 1−O−β−D−mannopyranosylerythritol as a hydrophilic headgroup and fatty acids and acetyl groups as the hydrophobic chain (Kitamoto 2008). MELs can be classified according to the their degree of acetylation (MEL−A; di−acetylated at the C−4 and C−6 positions of mannose, MEL−B; mono−acetylated at the C−6 position of mannose, MEL−C; mono−acetylated at the C−4 position of mannose, and MEL−D; deacetylated) (Fig 1) or according to the number of fatty acid chains (mono−acylated, di−acylated, and tri−acylated) and the chirality of mannosylerythritol (conventional and diastereomer) (Saika, Koike et al. 2018). MELs are produced by basidiomycetous yeast strains in the genera *Pseudozyma* (the majority of MEL−producing fungi) and *Ustilago* isolated from various vegetables such as sugarcane and leaves of *Perilla frutescens* (Morita, Konishi et al. 2007; Morita, Fukuoka et al. 2009; Konishi, Maruoka et al. 2014). MELs produced by most of these strains are mixtures consisting primarily of MEL−A along with smaller amounts of MEL−B, MEL−C, and MEL−D.

The first-known MEL producing fungus is *Pseudozyma antarctica*, which mainly produced MEL-A along with smaller amounts of MEL-B and MEL-C (Kitamoto, Haneishi et al. 1990). Since then, the development of new screening methods has led to discover numerous MEL-producing fungi and identify unknown MEL structures. It has been revealed that the structural diversity of MELs depends on the type of MEL-producing fungi and their substrates (Table 1). For instances, *Pseudozyma churashimaensis* produces MEL-A as the major product with minor fraction of monoactylated and triacetylated MELs (Morita, Ogura et al. 2011). *Pseudozyma tsukubaensis* and the snut fungus *Ustilago scitaminea* produce the diastereomer type of MEL-B (Morita, Takashima et al. 2010; Morita, Ishibashi et al. 2011). *Pseudozyma shanxiensis*, *Pseudozyma hubeiensis*, and *Ustilago cynodontis* are reported to produce mainly MEL-C (Fukuoka, Morita et al. 2007; Konishi, Morita et al. 2008; Morita, Konishi et al. 2008). MEL-D is only produced as a minor fraction in MEL mixtures and there have been no reports of natural strains capable of majorly producing MEL-D. In addition, the structural diversity of MELs produced based on various strains and substrates contribute to different properties of each MELs. MEL-B and MEL-C have higher hydrophilicity than MEL-A, which makes them more suitable for use in aqueous solutions. It has been reported that the diastereomer type of MEL-B produced by *Pseudozyma tsukubaensis* is commercialized as cosmetic ingredient (Saika, Koike et al. 2018).

The initial application of MELs is a biosurfactants, which are known to have excellent interfacial activity, biodegradability, biocompatibility, and environmentally friendly production process, compared to those derived from petroleum (Kitamoto, Yanagishita et al. 1993). Innovative ways to produce and modulate a desired form of MELs have been accelerated to date, and the applications of MELs in a wide range of industries such as cosmetics, pharmaceuticals, agriculture, and food have received much attention besides biosurfactant property (Morita, Tadokoro et al. 2011; Morita, Fukuoka et al. 2013; Mnif and Ghribi 2016). In particular, the various biological effects reported to date have provided the basic evidences for the effective use of MELs in the pharmaceutical industry. MELs are reported to exhibit anti-cancer, anti-inflammation, and anti-microbial and oxidative activities (Kitamoto, Yanagishita et al. 1993; Isoda, Kitamoto et al. 1997; Zhao, Wakamatsu et al. 1999; Im, Nakane et al. 2001; Morita, Tadokoro et al. 2011; Takahashi, Morita et al. 2012; Inoh, Furuno et al. 2013). In addition, MELs have attracted considerable interest in the cosmetics industry as the moisturizing activity of MELs was addressed using a three-dimensional cultured human skin model and human forearm skin (Morita, Kitagawa et al. 2009; Yamamoto, Morita et al. 2012). The recovery effect of MELs on damaged hair suggested its potential as a component of new hair-care products (Morita, Kitagawa et al. 2010). Anti-oxidant and protective effects of MELs against H_2O_2-

induced oxidative damage in the dermal fibroblasts could have potential as anti-aging ingredients (Takahashi, Morita et al. 2012).

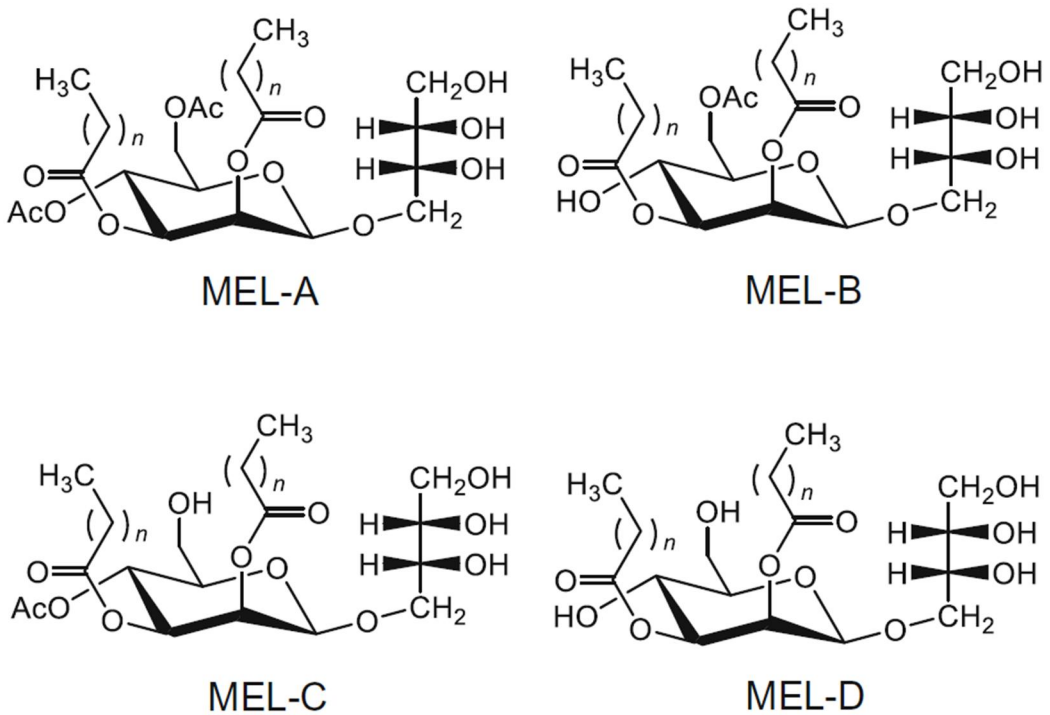

Fig 1. Chemical structures of MELs (Saika, Koike et al. 2018).

.

Strains	Structure of MEL	Carbon source
P. antarctica	MEL-A (as a main product), MEL-B, MEL-C, MEL-D	Vegetable oil
	Mono-acylated MEL	Glucose
	Tri-acylated MEL	Soybean oil
P. parantarctica	MEL-A (as a main product), MEL-B, MEL-C	Soybean oil
	Mono-acylated MEL	Glucose
	Tri-acylated MEL	Soybean oil
	Mannosylribitol lipid (MRL)	Olive oil, Ribitol
	Mannosyl-D-arabitol lipid (MDAL)	Olive oil, D-Arabitol
	Mannosyl-D-mannitol lipid (MDML)	Olive oil, D-Mannitol
P. aphidis	MEL-A (as a main product), MEL-B, MEL-C, MEL-D	Soybean oil
P. crassa	Diastereomer type of MEL-A, MEL-B, MEL-C	Soybean oil
P. tsukubaensis	Diastereomer type of MEL-B	Soybean oil
	Mannosyl-L-arabitol lipid (MLAL)	Olive oil, L-Arabitol
P. hubeiensis	MEL-C (as a main product), MEL-A, MEL-B	Soybean oil
P. shanxiensis	MEL-C	Soybean oil

Table 1. MELs produced by genus *Pseudozyma* (Saika, Koike et al. 2018)

Melanogenesis and MELs

Melanocytes, neural crest-derived cells located on the stratum basale of the skin epidermis, produces melanin through melanogenesis (Bonaventure, Domingues et al. 2013; D'Mello, Finlay et al. 2016). The normal level of melanin in the epidermis protects the skin against ultraviolet radiation (Brenner and Hearing 2008), but abnormal melanogenesis is associated with a variety of dermatological problems represented by hyperpigmentation or hypopigmentation. Melasma, solar lentigines, age spots, and pigmented acne scars are associated with hyperpigmentation (Andersen, Labadie et al. 1997; Ho, Yeung et al. 2011; Wu, Lambert et al. 2012; Yonei, Kaminaka et al. 2012), whereas vitiligo and albinism is linked with hypopigmentation (Malhotra and Dytoc 2013). Melanin synthesis is a complex process with multiple steps (Fig 2). Several melanogenic enzymes and catalytic reactions are involved in melanin synthesis (Ando, Kondoh et al. 2007; Pillaiyar, Namasivayam et al. 2018). Tyrosinase, tyrosinase-related protein-1 (Tyrp-1), and tyrosinase-related protein -2 (Tyrp-2, also known as dopachrome tautomerase) are essential regulators on the melanin synthesis in human as well as in murine melanocytes (Korner and Pawelek 1982; Kameyama, Sakai et al. 1995). Tyrosinase, only produced in melanocytes, is a glycoprotein with six N-linked glycosylation sites, functioning as the rate-limiting oxidase to directly control melanin synthesis (Ando, Kondoh et al. 2007). Tyrosinase oxidizes L-tyrosine and/or L-3,4-

dihydroxyphenylalanine (L-DOPA) to dopaquinone which serves as a substrate for synthesis of melanin. Tyrp-1 is reported to catalyze the oxidation of 5,6-dihydroxyindole-2-carboxylic acid (DHICA) to indol-5,6-quinone 2-carboxylic acid, and Tyrp-2 catalyzes the DOPAchrome to DHICA (Tsukamoto, Jackson et al. 1992; Kobayashi, Urabe et al. 1994). For this reason, the regulation of expression level of above-mentioned three melanogenic enzymes has been the focus of numerous whitening or anti-melanogenesis studies (Lee, Baek et al. 2018; Lee, Nam et al. 2018).

Microphthalmia-associated transcription factor (MITF) is a key transcription factor known to be essential for melanogenesis, and regulates the transcription of three forementioned major pigmentation enzymes by binding 11-base pair M box containing a CATGTG motif in their promoter sites (Yasumoto, Yokoyama et al. 1997). MITF also modulates differentiation, proliferation, survival and motility in melanocytes (Shibahara, Takeda et al. 2001; Levy, Khaled et al. 2006). Hypopigmentation or generalized depigmentation in the skin and hair is caused by mutation of MITF gene (Amiel, Watkin et al. 1998; Smith, Kelley et al. 2000). Oxidative stress induces down regulation of differentiated mRNA markers and reduces MITF gene expression, thereby inhibiting melanin production in melanocytes (Jimenez-Cervantes, Martinez-Esparza et al. 2001).

Activated p53 in UVR-irradiated keratinocytes induces transcription of proopiomelanocortin (POMC), which enzymatically degrades to produce several derivatives including α-melanocyte stimulating hormone (α-MSH). Induced α-MSH binds to MC1R on melanocytes, which activates adenylyl cyclase to induce adenosine 3',5'-monophosphate (cAMP) production and protein kinase A (PKA) activation. This, in turn, phosphorylates cAMP-responsive element binding (CREB) protein, followed by activation of the MITF-M promoter containing the cAMP response element (CRE) site (Hsiao and Fisher 2014; D'Mello, Finlay et al. 2016). MITF is also a target of the mitogen-activated protein kinase (MAPK) pathway (Hemesath, Price et al. 1998). A series of phosphorylation of extracellular signal–regulated kinase (ERK)/ribosomal s6 kinase (RSK)/CREB signaling molecules promote MITF activation (Imokawa and Ishida 2014). On the other hand, ERK is reported to negatively regulate melanogenesis by degradading MITF (Wu, Hemesath et al. 2000; Xu, Gong et al. 2000).

There are a few reports to examine the effect of MELs (composed of mainly MEL-A) on B16 melanoma cells. In their reports, MELs mediated B16 melanoma cell apoptosis, which was associated with growth arrest in the G1 phase (Zhao, Wakamatsu et al. 1999) and the endoplasmic reticulum stress (Fan, Li et al. 2016). Studies using MELs including MEL-B or MEL-C as the main products have not been reported yet.

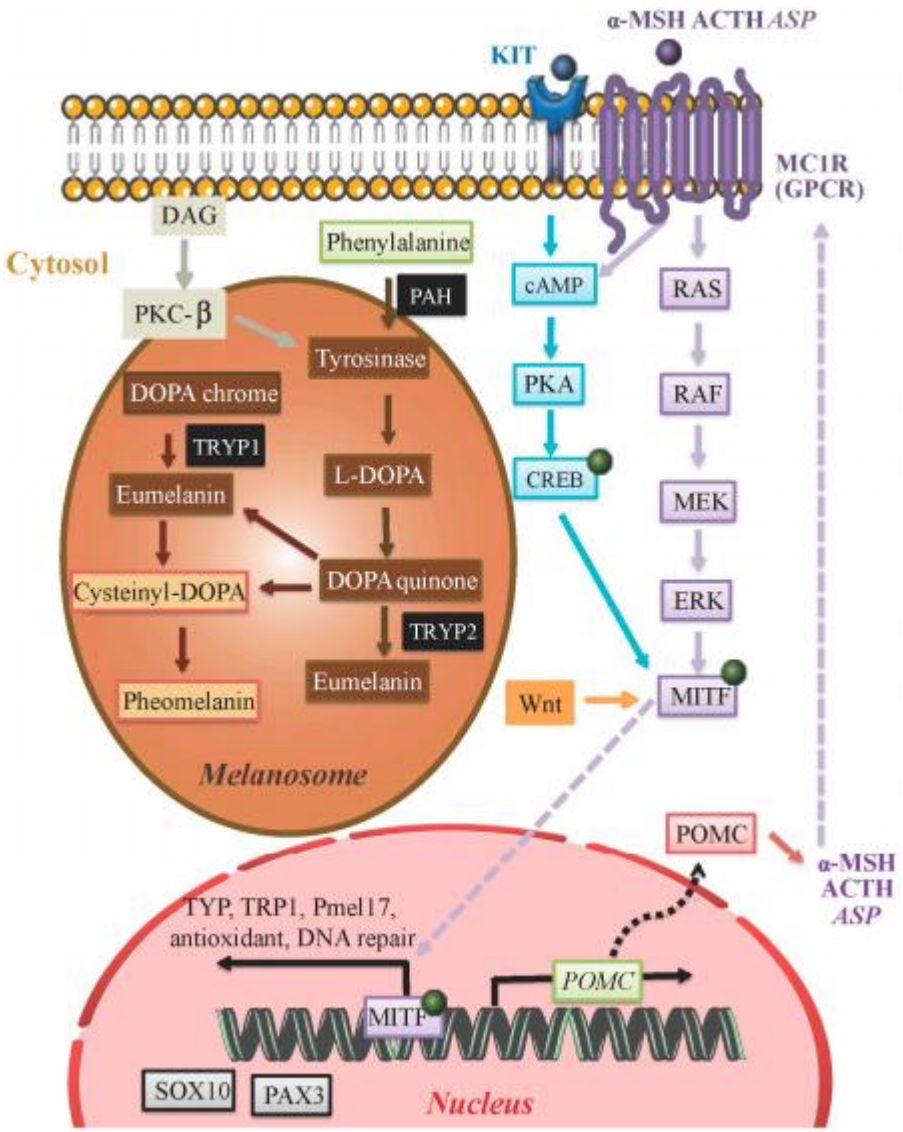

Fig 2. Schematic of melanin synthesis catalyzed by essential melanogenic enzymes and regulated by a series of signaling pathways (D'Mello, Finlay et al. 2016).

Moisturization and MELs

Disorganization and/or damage of the lipid matrix in the stratum corneum (SC), which accounts for 20% of the SC volume, leads to a decrease in water-retention properties and a marked increase transepidermal water loss (TEWL), impairing skin moisturization (Elias and Menon 1991; Leveque, de Rigal et al. 1993; Wertz and van den Bergh 1998; Harding 2004). Since MELs are a type of functional glycolipid, as mentioned above, there have been a few studies to confirm the skin moisturizing effect using the physicochemical properties of lipid components (Morita, Kitagawa et al. 2009; Yamamoto, Morita et al. 2012). MELs (MEL-A as a main product) showed recovery effect on the viability of sodium dodecyl sulfate (SDS)-damaged human skin cells in a three-dimensional cultured human skin model, TESTSKIN^{TM} (Toyobo, Japan), suggesting the potential moisturizing ability (Morita, Kitagawa et al. 2009). In addition, topical application of MELs (MEL-B as a main product) to human forearm skin showed increased level of water-retention and decreased level of TEWL for approximately 2 hours (Yamamoto, Morita et al. 2012).

Aquaporin-3 (AQP3), the most well-investigated AQP in the skin, is a transporter of water, glycerol, and other small solutes expressed in plasma membrane of keratinocytes in the epidermal basal layer (Hara-Chikuma and Verkman 2008). AQP3 deficiency is reported to be associated with decreased SC hydration (Hara, Ma et al. 2002; Ma, Hara

et al. 2002; Hara and Verkman 2003). These results provide scientific evidences for the development of ingredients that preserve or enhance AQP3 expression in the cosmetics and cosmeceutical industries. For example, UVB-irradiation was reported to downregulate AQP3 expression by activating the MEK/EKR pathway in cultured human keratinocytes. (Cao, Wan et al. 2008). Several studies have been conducted to identify substances that can recover AQP3 downregulation induced by UVB-irradiation (Ji, Yang et al. 2010; Jeon, Kang et al. 2015). However, Verkman suggested that full considerations should be given to the development of AQP3 enhancement products for effective skin moisturization based on the studies of excessive expression of epidermal AQP3 and skin tumorigenesis (Yuspa, Dlugosz et al. 1996; Hara-Chikuma and Verkman 2008; Verkman 2008).

Summary

As the applicability of MELs increases in various industrial fields and the production technologies advance, it is also becoming possible to produce customized MELs. The use of MELs is anticipated to increase in the cosmetics, cosmeceutical, and pharmaceutical industries in the upcoming future. In particular, since MELs including MEL-B as a main composition is highly hydrophilic and has been proved to have potential to be commercialized in the cosmetics, further efforts will be required to demonstrate their effectiveness and the action of mechanisms that has not been elucidated.

In the present study, I aimed to reveal yet-unknown biological efficacies of MELs which are composed of 85% di-acylated MEL-B and 15% tri-acylated MEL. I believed that this study would be meaningful because there have been few reports demonstrating efficacy of MELs consisting of 85% di-acylated MEL-B and 15% tri-acylated MEL on whitening and moisturization. In addition, I attempted to demonstrate underlying mechanisms for skin whitening and moisturizing using *in vitro* human skin cells and a three-dimensional human skin equivalent for strengthening the value of this study.

CHAPTER I.

MANNOSYLERYTHRITOL LIPIDS INHIBIT MELANOGENESIS VIA SUPPRESSING ERK-CREB-MITF-TYROSINASE SIGNALING IN NORMAL HUMAN MELANOCYTES AND A THREE-DIMENSIONAL HUMAN SKIN EQUIVALENT

Abstract

Hyperpigmentation is caused by excessive production of melanin in melanocytes. MELs are extracellular glycolipid biosurfactants that are abundantly produced by yeasts and commercially used in cosmetics. However, the potential depigmenting efficacy of MELs has not been evaluated. In the present study, the depigmentary effect of MELs was investigated in primary normal human melanocytes (NHMs), α-melanocyte-stimulating hormone (MSH)-stimulated B16 cells (murine melanoma cells), and a three-dimensional human skin equivalent (MelanoDerm^{TM}) using photography, hematoxylin & eosin (H&E) staining, Fontana-Masson (F&M) staining, and two-photon excitation microscopy. MELs significantly decreased the melanin contents in NHMs and α-MSH-stimulated B16 cells. Consistent with these findings, Treatment of MELs had a clear whitening effect in a three-dimensional human skin equivalent, brightening the tissue color and reducing the melanin content. The molecular mechanism underlying the anti-melanogenic effect of MELs treatment was examined by real-time qRT-PCR and western blotting. Mechanistically, MELs clearly suppressed the gene expression levels of representative melanogenic enzymes, including tyrosinase, Tyrp-1, and Tyrp-2, by inhibiting the ERK/CREB/MITF signaling pathway in NHMs. This work demonstrates for the first time that MELs exert whitening effects on human melanocytes and skin equivalent. Thus, I suggest that MELs could be developed as a potent anti-melanogenic

agent for effective skin whitening, beyond their original use as a biosurfactant in cosmetics.

Introduction

MELs are a class of glycolipid biosurfactants produced by various strains of yeast and fungi (Zhao, Wakamatsu et al. 1999). These features of MELs make them attractive for application in various areas. For example, yeast glycolipid biosurfactants have been shown to moisturize dry skin, repair damaged hair, activate fibroblasts and papilla cells, and exert anti-oxidative and protective effects in skin cells, making them a practical choice for use in cosmetics (Morita, Fukuoka et al. 2013).

Melanogenesis is the process of melanin production. As the overproduction of melanin causes deteriorative forms of melanin hyperpigmentation, such as freckles and lentigo (Briganti, Camera et al. 2003), many researchers have focused on developing effective depigmentary ingredients for cosmetics or medicines. However, few such agents have proved satisfactory in their safety and efficacy.

Tyrosinase is a rate-limiting enzyme in melanogenesis (Plonka, Handjiski et al. 2006), and inhibition of its activity or expression is often employed to treat hyper-pigmentation. MITF is a transcription factor that is important for the expression of melanogenic enzymes, such as tyrosinase, Tyrp-1, and Tyrp-2 (Yasumoto, Yokoyama et al. 1995). MITF expression is mainly induced by CREB, which is activated by the PKA signaling pathway (Lee, Jang et al. 2013). In addition, the serial phosphorylation (activation) of mitogen-activated protein kinase kinase (MEK), ERK1/2, and RSK increases MITF gene expression via the

phosphorylation of CREB (Grewal, Fass et al. 2000; Imokawa and Ishida 2014). Interestingly, the activation of MEK/ERK/RSK also induces the phosphorylation and degradation of MITF, ultimately suppressing melanogenesis (Kim, Hwang et al. 2003).

In the present study, I demonstrate for the first time that MELs inhibit melanin synthesis in primary NHMs and α-MSH-stimulated B16 mouse melanoma cells. Mechanistically, it is shown that MELs significantly suppress the gene expression of melanogenic enzymes via inhibition of the ERK/CREB/MITF signaling pathway. Finally, it is revealed that MELs have marked whitening effects in a three-dimensional human skin equivalent system (MelanoDerm^{TM}), as assessed using photography, histological tissue staining, and two-photon excitation microscopy. Collectively, the present results from the current experiment suggested that MELs have important whitening effects in human experimental systems.

Materials and Methods

MELs preparation

The biosurfactant MELs used in this study were synthesized by the yeast, *Pseudozyma* sp. The MELs were extracted from the culture broth using ethyl acetate and purified by a fatty acid removal process. They were produced and provided by DKBIO (Daejeon, South Korea), had a purity of 95%, and comprised 85% di-acylated MEL-B and 15% tri-acylated MELs.

Cell culture

Primary NHMs from the neonatal foreskin of a darkly pigmented donor were purchased from Cascade Biologics (#C2025C; Portland, OR, USA) and cultured in Medium 254 (#M-254-500; Cascade Biologics) supplemented with Human Melanocyte Growth Supplement (HMGS-2, S-016-5; Cascade Biologics). For experiments, primary NHMs were used between passages 4 and 7. B16 murine melanoma cells, Dulbecco's modified Eagle's medium (DMEM), and fetal bovine serum (FBS) were purchased from the American Type Culture Collection (ATCC; Manassas, VA, USA). Cells were cultured in DMEM containing 5% FBS with incubation at 37°C under a 10% CO_2 atmosphere.

Cell viability assay

Cell viability was determined using a Cell Counting Kit-8 (CCK-8; CK04-05, Dojindo, Japan) as described by the manufacturer. Briefly, primary NHMs and B16 murine melanoma cells seeded to a 96-well plate at a density of 5×10^3 cells/well were incubated with MELs for 24 h. Then, 10 $\mu\ell$ of CCK-8 solution and 90 $\mu\ell$ of DMEM (#31053-028, ThermoFisher Scientific, Waltham, MA, USA) were added to each well and the plate was incubated at 37°C for 2 h. The absorbance was measured at 450 nm using a microplate reader (Synergy2, BioTek, Winooski, VT, USA).

Measurement of melanin content

Melanin contents were determined as described in the previous report (Lee, Lee et al. 2017). Briefly, NHMs were treated with the indicated concentrations of MELs for 5 d. B16 cells were treated with the indicated concentrations of MELs and α-MSH (200 nM) for 3 d. Thereafter, all cells were washed with phosphate-buffered saline (PBS; 21-031-CVR, Corning, USA) and lysed with 1N NaOH at 60°C for 1 h. The cell lysates were transferred to a 96-well plate, and absorbance was measured at 405 nm using a microplate reader. The total protein content in each experimental group was measured using a DC Protein Assay kit (BioRad, Hercules, CA, USA). The calculated melanin content in each experimental group was expressed relative to the total protein content.

Cellular tyrosinase activity assay

Total cellular tyrosinase activity was determined as described in the previous report (Delijewski, Wrzesniok et al. 2016). In the current study, total cellular tyrosinase activity in α-MSH-stimulated B16 cells was determined by measuring the rate of oxidation of L-DOPA to dopachrome. Cell lysates were purified by centrifugation at 13,000 rpm for 5 min. A tyrosinase substrate, L-DOPA (2 mg/ml), was prepared in the phosphate buffer. 100 ㎕ of each lysate was added to a 96-well plate, and 40 ㎕ of L-DOPA solution was added, and enzyme analysis was started at 37 ° C. For the control, 100 ㎕ of lysis buffer and 40 ㎕ of L-DOPA solution were added. Absorbance of dopachrome was measured at 475 nm using a microplate reader. 100 ㎍/㎖ of kojic acid (KA; K3125, St. Louis, MO, USA) was used as a reference compound. The result of cellular tyrosinase activity was expressed as the percentage of the controls.

Mushroom tyrosinase activity assay

A cell-free assay system was used to investigate the direct effects of the indicated concentrations of MELs on tyrosinase activity. Briefly, 100 ㎕ of phosphate buffer containing MELs were mixed with 10 units of mushroom tyrosinase (T3824, Sigma) and combined with 50 ㎕ of 0.03% L-tyrosine in distilled water. The mixture was incubated at 37°C for 10 min, and absorbance was measured at 405 nm. 5 ㎍/㎖ of KA was used

as a reference compound. The result of mushroom tyrosinase activity was expressed as the percentage of the controls.

RNA isolation and real-time quantitative reverse transcription-polymerase chain reaction (qRT-PCR)

Total RNA was extracted from cells using the TRIzol reagent (Invitrogen, Grand Island, NY, USA), and cDNA was prepared using a RT-premix (Bioneer, Seoul, South Korea). qRT-PCR was performed using an Applied Biosystems 7500 Fast real-time PCR system (Applied Biosystems, CA, USA). The pre-inventoried TaqMan™ primer sets for tyrosinase (Hs00165976_m1), Tyrp-1 (Hs00167051_m1), Tyrp-2 (Hs01098278_m1), MITF (Hs01117294_m1), and TaqMan™ Gene Expression Master Mix (#4369016) used for amplification were purchased from Applied Biosystems. Target gene expression was normalized against that of the housekeeping gene encoding ribosomal protein lateral stalk subunit P0 (RPLP0; Hs99999902_m1). Relative quantization was performed using the comparative ΔΔCt method according to the instructions provided with the manufacturer's instructions.

Western blotting

NHMs were washed twice with cold PBS and then lysed in ice-cold modified RIPA buffer (50 mM Tris-HCl, pH 7.4, 1% Nonidet P-40, 0.5% sodium deoxycholate, and 150 mM NaCl) containing protease inhibitors

and a phosphatase inhibitor cocktail (Calbiochem, San Diego, CA, USA). Equal amounts of protein (30 ㎍/well) were loaded, separated by SDS-polyacrylamide gel electrophoresis (SDS-PAGE), and transferred to nitrocellulose membranes (LC2000, Invitrogen, USA). The membranes were incubated at 4℃ for 24 h with each of the following primary antibodies: MITF (ab20663, Abcam), beta-actin (#4970, Cell Signaling Technology), CREB (#4820, Cell Signaling Technology), p-CREB (#9198, Cell Signaling Technology), ERK (#4695, Cell Signaling Technology), p-ERK (#4370, Cell Signaling Technology), AKT (#4691, Cell Signaling Technology), p-AKT (#4060, Cell Signaling Technology), PKA (#5842, Cell Signaling Technology), and p-PKA Substrate (#9624, Cell Signaling Technology). After three washes with tris-buffered saline containing 0.1% Tween-20 (TBST), the membranes were exposed to horseradish peroxidase-conjugated secondary antibodies for 1 h at room temperature, washed, and then detected using an Enhanced Chemiluminescence (ECL) Prime detection reagent kit (RPN2232, GE Healthcare, UK). Chemiluminescent signals were visualized using a chemiluminescent detection system (LAS-3000, Fuji Film, Japan). Densitometric analysis for Western blot band was performed using the NIH ImageJ software.

Three-dimensional human skin equivalent and histology

As a human skin tissue equivalent model, I used MelanoDerm^{TM} (MEL-

300-B; MatTek Corp., Ashland, MA, USA). This viable reconstituted three-dimensional human skin equivalent was derived from black donors and contains normal melanocytes and keratinocytes. MelanoDerm™ was maintained in EPI-100-NMM-113 medium from MatTek as recommended by the manufacturer. Prior to MELs treatment, tissues were washed with 1 ml of PBS to remove any residual compounds. MELs were dissolved in dimethyl sulfoxide (DMSO, #471267, Sigma) to 100 mg/ml and further diluted in PBS. The final concentrations of MELs were 0.3 mg/ml (0.03%) and 1 mg/ml (0.1%). Control sample was treated with PBS containing 1% DMSO. MELs were applied to the MelanoDerm™ on days 1, 4, 6, 8, 11, 13, and 15. On day 18, the MelanoDerm™ tissues were fixed in 4% buffered formaldehyde, embedded in paraffin, cut to a thickness of 4 ㎛, and subjected to hematoxylin and eosin (H&E) staining and Fontana-Masson (F&M) staining. The viability of tissue sample was assessed using a Cell Counting Kit-8 (CCK-8) as described by the manufacturer (Dojindo, Tokyo, Japan).

Two-photon excitation fluorescence (TPEF) imaging

For TPEF imaging, I used a *fs*-pulsed Ti:sapphire laser (Chameleon Vision-S; Coherent Inc., Santa Clara, CA, USA) capable of tuning wavelengths from 690 nm to 1050 nm with a pulse width of 75 *fs* and a repetition rate of 80 MHz. The laser beam was delivered into an inverted microscope (FV1000MPE +IX81; Olympus, Tokyo, Japan). To visualize

the distribution of melanin in the three-dimensional human skin equivalent, I used an excitation wavelength of 800 nm and collected emitted backward signals at wavelengths of 490 to 540 nm using a bandpass filter. A 60x water-immersion UPlanSApo/UIS2 objective lens (numerical aperture [NA] 1.2; Olympus, Tokyo, Japan) was used to focus the laser beam into the sample. For sample preparation, each MelanoDerm^{TM} preparation was fixed in 4% formalin for 24 h at 4° C, and then washed with PBS/0.1% BSA (bovine serum albumin). The basement membrane sides of the MelanoDerm^{TM} sample were imaged to measure intracellular melanin in the melanocyte layer. The measurement volume was 200 (x) x 200 (y) x 60 (z) μm^3, and 61 image slices (z-depth interval = 1 μm) were reconstructed to produce each three-dimensional image. The relative TPEF signal intensities for melanin in the measurement volume were quantified using the Image-Pro Premier three-dimensional software (Media Cybernetics, Inc., Bethesda, MD, USA).

Statistical analysis

All data are expressed as means ± SD (standard deviation), and the Student's t-test was used for statistical comparisons. A p-value < 0.05 was considered statistically significant.

Results

MELs significantly inhibit melanin synthesis in normal primary melanocytes

Prior to examining the anti-melanogenic efficacy of MELs, I determined their cytotoxicity in NHMs. As shown in Fig 3A, MELs did not show any cytotoxicity at concentrations below 5 ㎍/ml, but rather slightly increased cell viability. Next, I treated NHMs with 1, 2, and 5 ㎍/ml MELs for 5 days. As shown in Fig 3B, MELs dose-dependently decreased the intracellular melanin content of NHMs and brightened the color of lysates obtained from these cells. To further confirm the anti-melanogenic ability of MELs, I used α-MSH-stimulated B16 cells, which are commonly used to test depigmenting efficacy in vitro. MELs had no cytotoxicity against α-MSH-stimulated B16 cells at concentrations up to 10 ㎍/ml (Fig 4A). Consistent with the results I obtained in NHMs, MELs dramatically suppressed the extracellular and intracellular melanin contents of α-MSH-stimulated B16 cells (Fig 4B). Therefore, I conclude that MELs significantly inhibit melanin synthesis in melanocytes.

A

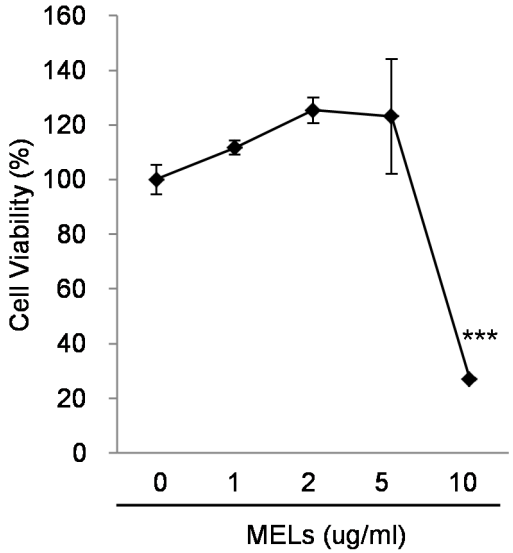
160
140
120
100
80
60
40
20
0
Cell Viability (%)
***
0
1
2
5
10
MELs (ug/ml)

B

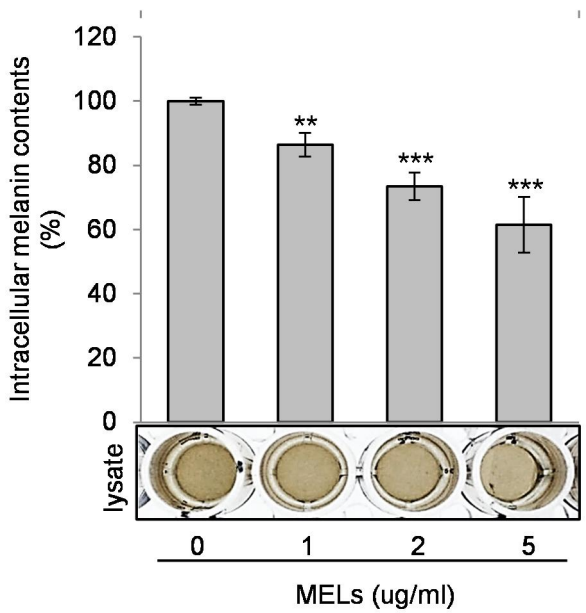
120
100
80
60
40
20
0
Intracellular melanin contents (%)
**
***
***
lysate
0
1
2
5
MELs (ug/ml)

Fig 3. Anti-melanogenic effect of MELs in NHMs. NHMs were treated with the indicated concentrations of MELs for 5 days. (A) Effects of MELs on the viability of NHMs. (B) Effects of MELs on melanin synthesis in NHMs. NHMs were treated with the indicated concentrations of MELs for 5 days, and washed, and lysed with NaOH to determine the intracellular melanin contents. The melanin contents were estimated by absorbance at 405 nm. The photographs show the colors of lysates obtained from control and MELs-treated cells. Data are expressed as the mean ± SD of at least three independent measurements and a percentage of the results obtained from untreated cells (*$p < 0.05$, **$p < 0.01$, ***$p < 0.001$).

A

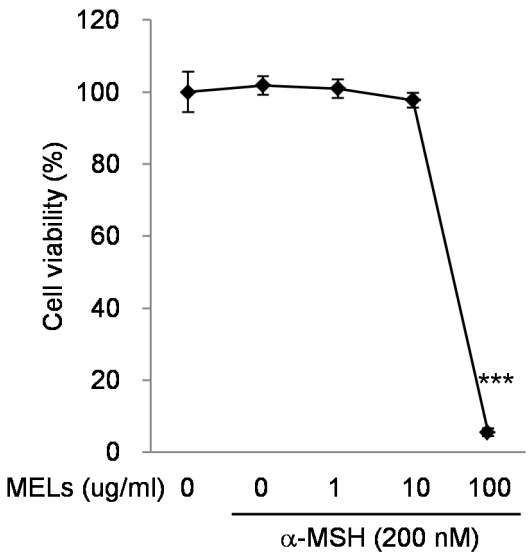
120
100
80
60
40
20
0
Cell viability (%)
***
MELs (ug/ml) 0
0
1
10
100
α-MSH (200 nM)

B

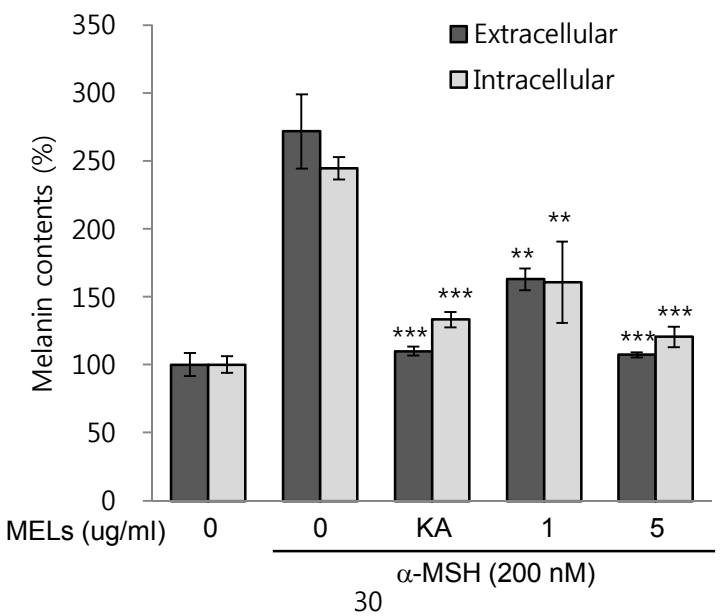
350
300
250
200
150
100
50
0
Melanin contents (%)
Extracellular
Intracellular
***
**
MELs (ug/ml)
0
0
KA
1
5
α-MSH (200 nM)

Fig 4. Anti-melanogenic effect of MELs in α-MSH-stimulated B16 murine melanoma cells. B16 cells were treated with the indicated concentrations of MELs and α-MSH for 3 days. (A) Effects of MELs on the viability of α-MSH-stimulated B16 cells. (B) Extracellular and intracellular melanin contents in α-MSH-stimulated B16 cells. Extracellular melanin contents were determined using cultured media containing secreted melanin after MELs and α-MSH co-treatment for 3 days. Intracellular melanin contents were determined using cell lysates, as described in method section. The melanin contents were estimated by absorbance at 405 nm and normalized by the total protein contents. KA indicates kojic acid (100 μg/ml), which was used as a reference compound. Data are expressed as the mean ± SD of at least three independent measurements and a percentage of the results obtained from untreated cells (*$p < 0.05$, **$p < 0.01$, ***$p < 0.001$).

MELs exert a whitening effect in a three-dimensional human skin equivalent through an inhibition of melanin synthesis

I next tested whether MELs could exert a whitening effect on the three-dimensional human skin equivalent, MelanoDerm^{TM} (MEL-300-B), which closely resembles human skin in its architecture and composition. MELs were topically applied to MelanoDerm^{TM} samples for 18 days at concentrations of 0.03% and 0.1%. Thereafter, I observed the cell viability, color, and melanin content of the tissues. As shown in Fig 5A, MELs-treated tissues did not exhibit any apparent cytotoxicity. Visual inspection and photography revealed that both 0.03% and 0.1% MELs-treated samples appeared lighter than PBS-treated control tissues after 18 days (Fig 5B). H&E staining revealed that MELs treatment did not induce any toxicity in the skin equivalent tissues, while F&M staining showed that MELs treatment was associated with decreases in the melanin content of melanocytes in the basal layer of the epidermis (Fig 5C, red color box). To further examine the change in melanin content, I compared the auto-fluorescence signals of melanin in the melanocyte layers of control and MELs-treated tissues using TPEF microscopy, as shown in Fig 5D. Indeed, the TPEF signal intensity for melanin in the melanocyte-rich area was apparently decreased in MELs-treated tissues compared with control tissues (Fig 5E). Taken together, my data indicate that, consistent with previous findings in NHMs and α-MSH-stimulated B16 cells, MELs exert a whitening effect in a three-

dimensional human skin equivalent, and this occurs through an inhibition of melanin synthesis.

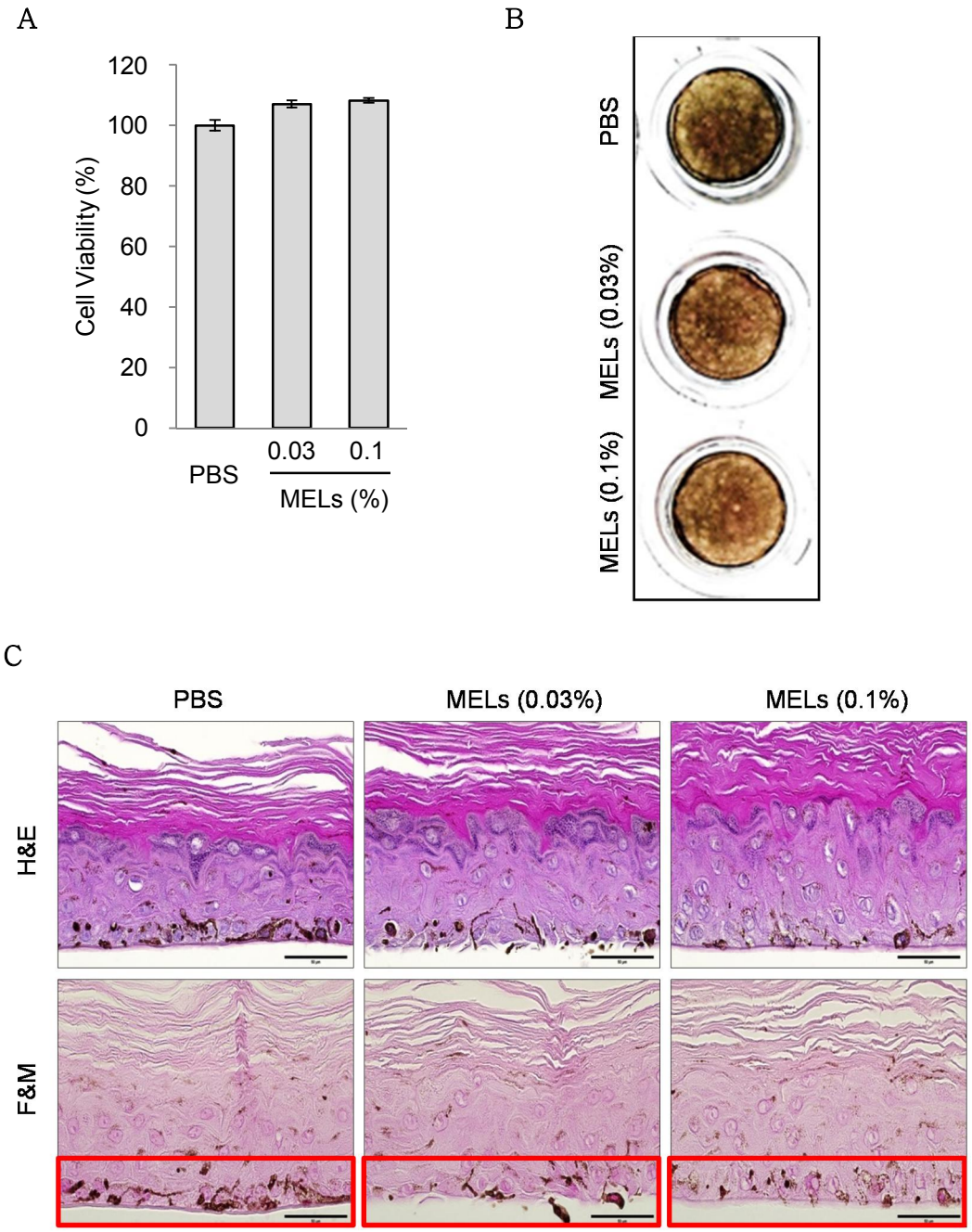

D

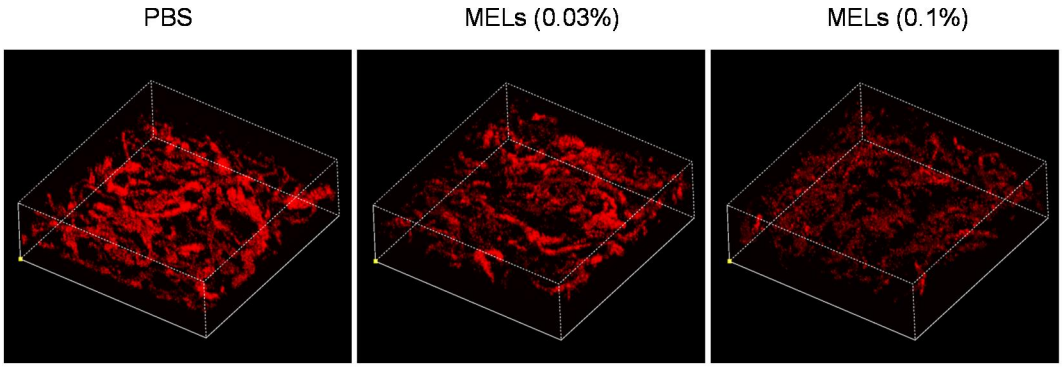
PBS
MELs (0.03%)
MELs (0.1%)

E

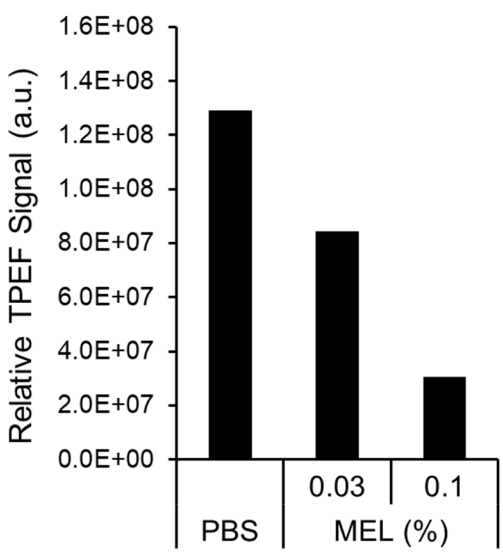
Relative TPEF Signal (a.u.)
1.6E+08
1.4E+08
1.2E+08
1.0E+08
8.0E+07
6.0E+07
4.0E+07
2.0E+07
0.0E+00
0.03
0.1
PBS
MEL (%)

Fig 5. (A) Viability of three-dimensional human skin equivalents treated with MELs. (B) Human skin equivalents (MelanoDerm^{TM}; n = 3) were treated with the indicated concentrations of MELs for 18 days, and then photographed. (C) H&E and F&M staining of tissue sections. The human skin equivalents were fixed in formaldehyde solution, embedded in paraffin wax, and sectioned for staining. The square red box shows the stained melanocytes in the basement layer (scale bar, 50 ㎛). (D) Melanin imaging (200 x 200 x 60 ㎛^{3}) of human skin equivalents was performed using TPEF microscopy. Pseudo-colored (red) signals indicate melanin (scale bar, 50 ㎛). (E) Quantification of TPEF signals in melanin-rich areas.

MELs suppress melanogenesis by decreasing the expression of tyrosinase

To begin defining the action mechanism of MELs, I next tested their inhibitory effect on tyrosinase activity. First, I performed the total cellular tyrosinase activity after MELs treatment in α-MSH-treated B16 cells. In Fig 6A, MELs significantly inhibited total cellular tyrosinase activity in α-MSH-treated cells. Then, I determined whether the inhibitory effect of MELs on tyrosinase is direct through a mushroom tyrosinase assay. As shown in Fig 6B, however, I found that MELs had no inhibitory effect on mushroom tyrosinase activity. Based on above data, I supposed that the decreased total cellular tyrosinase activity by MELs treatment may be caused by the decreased level of tyrosinase expression, but not direct inhibition of tyrosinase activity.

A

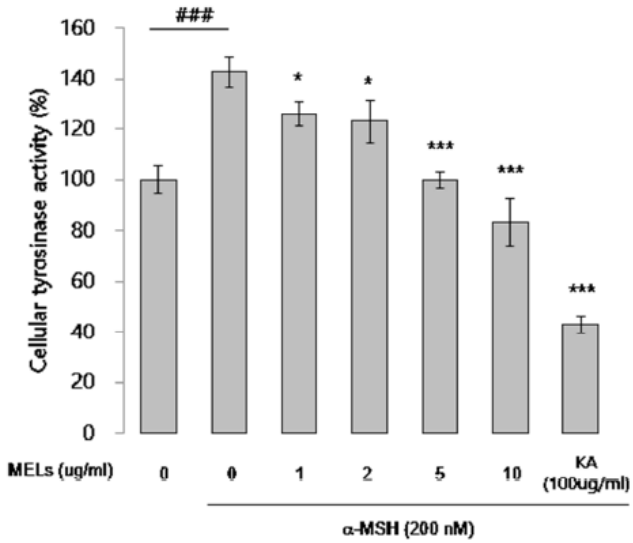
###
160
140
120
100
80
60
40
20
0
Cellular tyrosinase activity (%)
*
*
***
***
***
MELs (ug/ml)
0
0
1
2
5
10
KA
(100ug/ml)
α-MSH (200 nM)

B

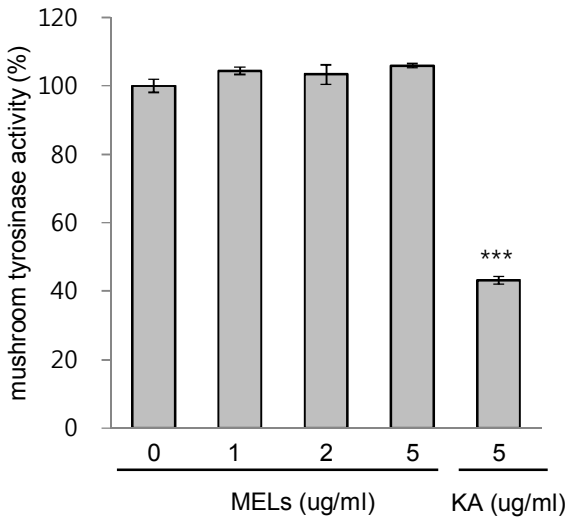
120
100
80
60
40
20
0
mushroom tyrosinase activity (%)
***
0
1
2
5
5
MELs (ug/ml)
KA (ug/ml)

Fig 6. Inhibitory effects of MELs on total cellular and cell-free tyrosinase activity. (A) B16 cells were treated with the indicated concentrations of MELs and α-MSH for 3 days. Then, I performed the cellular tyrosinase activity according to the method described in the Materials and Methods. (### $p < 0.001$ vs non-treated group, *$p < 0.05$ and ***$p < 0.001$ vs only α-MSH-treated group). (B) Effects of MELs on *in vitro* mushroom tyrosinase activity, as assessed in cell-free assays.

MELs suppress melanogenic gene expression through the inhibition of ERK-mediated CREB/MiTF signaling

I then further used real-time qRT-PCR to detect the gene expression levels of melanogenic enzymes (tyrosinase, Tyrp-1, and Tyrp-2) in MELs-treated NHMs. As shown in Fig 7A, MELs treatment significantly and time-dependently decreased the transcript levels of tyrosinase, Tyrp-1, and Tyrp-2, as assessed at 24, 48, and 72 h post-treatment. When I observed the protein and mRNA levels of MITF, which is a master transcription factor responsible for the gene expression of melanogenic enzymes, I found that MITF protein (Fig 7B) and mRNA (Fig 7C) expression levels were clearly inhibited by treatment of NHMs with MELs for 24 h. As these results suggested that MELs might inhibit melanogenic gene expression by suppressing MITF gene expression, I examined the protein level of phospho-CREB, which is known to critically regulate MITF gene expression (Lee, Jang et al. 2013). Indeed, I found that MELs treatment strongly decreased CREB phosphorylation (Fig 7D). I thus used Western blotting to further examine the activation of signaling molecules upstream of CREB phosphorylation, including PKA, AKT, and ERK (Lee, Jang et al. 2013; Imokawa and Ishida 2014). The results are shown in Fig 7E and 7F. MELs did not affect the phosphorylation of a PKA substrate, indicating that PKA activity is not inhibited by MELs treatment in NHMs. AKT phosphorylation was not almost changed by MELs, although a slight inhibition of phospho-AKT

was observed at 0.5 h after MELs treatment. However, ERK phosphorylation was dramatically, significantly and time-dependently decreased by MELs treatment. These data support the notion that MELs suppress melanogenic gene expression through the inhibition of ERK-mediated CREB/MITF signaling.

A

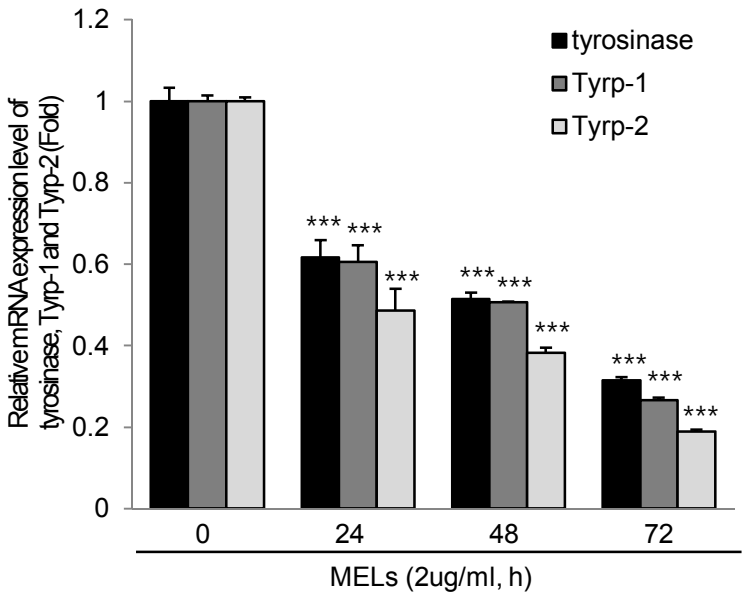
1.2
1
0.8
0.6
0.4
0.2
0
Relative mRNA expression level of tyrosinase, Tyrp-1 and Tyrp-2 (Fold)
tyrosinase
Tyrp-1
Tyrp-2
***
0
24
48
72
MELs (2ug/ml, h)

B

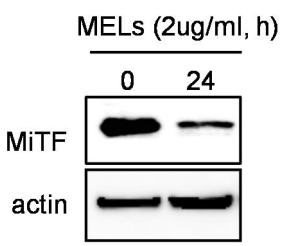
MELs (2ug/ml, h)
0
24
MiTF
actin

C

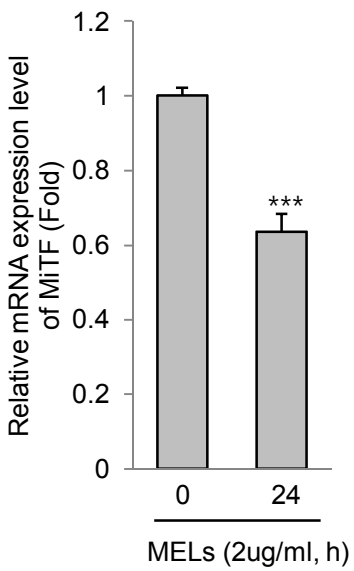
1.2
1
0.8
0.6
0.4
0.2
0
Relative mRNA expression level of MiTF (Fold)
***
0
24
MELs (2ug/ml, h)

D

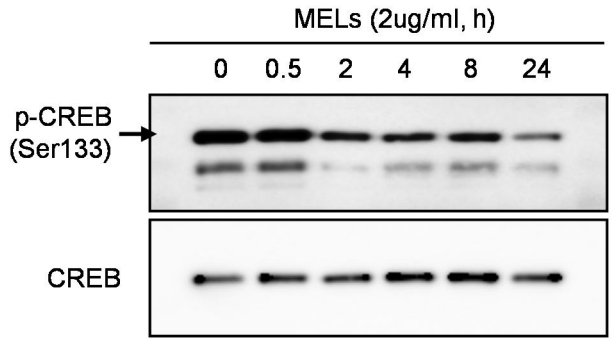
MELs (2ug/ml, h)
0
0.5
2
4
8
24
p-CREB
(Ser133)
CREB

E

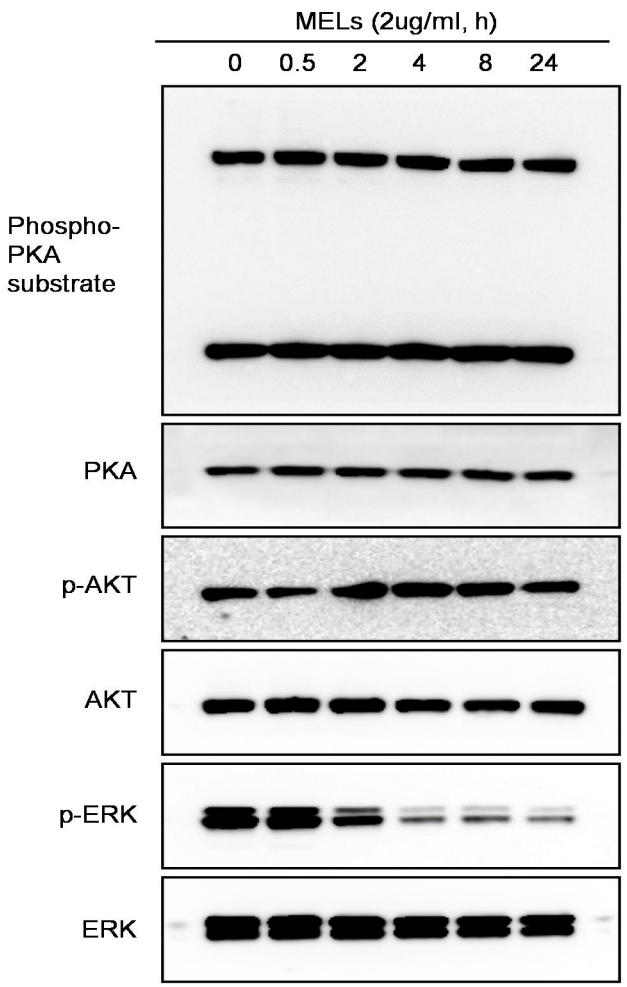
MELs (2ug/ml, h)
0
0.5
2
4
8
24
Phospho-
PKA
substrate
PKA
p-AKT
AKT
p-ERK
ERK

F

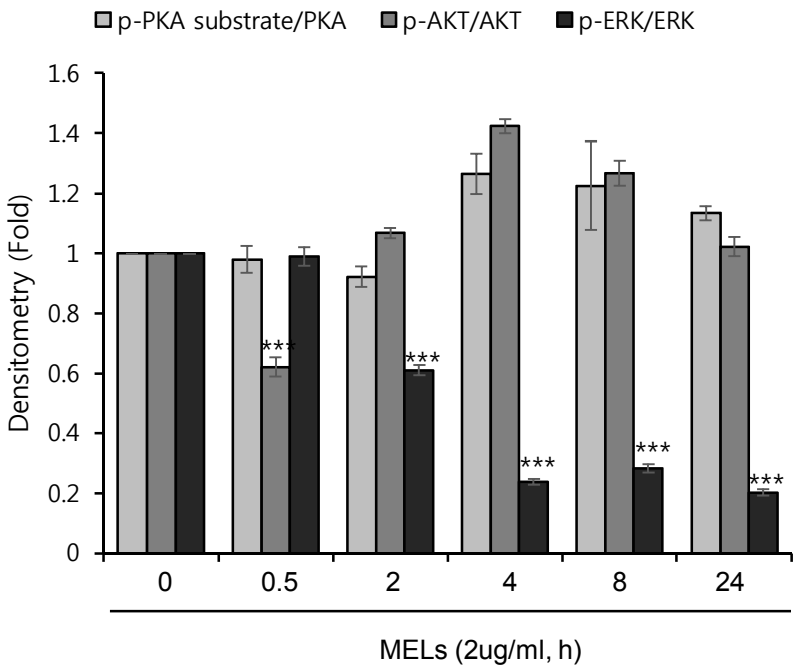

Fig 7. (A) Effects of MELs on the levels of melanogenic gene expression in NHMs. NHMs were incubated with 2 ㎍/ml MELs for the indicated times, and qRT-PCR was used to determine the gene expression levels of tyrosinase, Tyrp-1, and Tyrp-2. The graph indicated the fold of mRNA expression levels of target genes normalized by RPLP0 expression, as a reference gene. (B and C) Effects of MELs on the protein and transcript levels of MITF in NHMs. NHMs were incubated with 2 ㎍/ml MELs for 24 h. (B) Western blot analysis of the protein levels of MITF. (C) qRT-PCR analysis of the gene expression levels of MITF. The graph indicated the fold of mRNA expression level of MITF

gene normalized by RPLP0 expression, as a reference gene. (D and E) NHMs were incubated with 2 μg/ml MELs for the indicated times, and Western blotting was used to determine the protein levels of phospho-CREB/CREB, phospho-PKA substrate/PKA, phospho-AKT/AKT, and phospho-ERK/ERK. (F) Densitometric analysis was performed using the NIH ImageJ software. Data are expressed as the mean ± SD of at least three independent measurements ($*p < 0.05$, $**p < 0.01$, $***p < 0.001$).

Discussion

In the present study, I investigated new effects of MELs on whitening using in vitro human skin cells and a three-dimensional human skin equivalent. Although MELs are used as the commercial cosmetic ingredient, there are few their abilities for melanogenesis. According to the previous report (Zhao, Wakamatsu et al. 1999), the researchers found that the treatment of malignant melanoma B16 cells with MELs resulted in both apoptosis and differentiation in B16 cells, inducing significant tyrosinase activity and enhanced production of melanin. Ironically, their result is a contrast to our present data. However, I found differences that the composition of MELs they used is MEL-A (54%): MEL-B (25%): MEL-C (14%): MEL-D (7%), whereas the composition of MELs used in the present study is 85% di-acylated MEL-B and 15% tri-acylated MEL, as described in Materials and Methods. Namely, the composition rate and kinds of subtypes of MELs used in experiments may differently affect the melanin synthesis in melanocytes. It is very interesting for MELs to oppositely exert their effects on skin such as pigmentation or depigmentation, depending on the composition rate and subtypes of them. Therefore, I considered that the production condition of MELs complex may be crucial point for the development of effective cosmetics using the formulation possessing MELs to control skin physiology.

Furthermore, the present report provided a mechanism to account for the anti-melanogenic effect of MELs. It was elucidated that MELs decreased the gene expression of melanogenic enzymes through suppression of ERK/CREB/MITF signaling pathway. In fact, ERK phosphorylation by depigmenting compounds can induce MITF phosphorylation and degradation, ultimately suppressing melanogenesis (Kim, Hwang et al. 2003). However, simultaneously, ERK phosphorylation can induce MITF gene expression through CREB phosphorylation (Grewal, Fass et al. 2000; Imokawa and Ishida 2014). Overall, ERK activation can ambilaterally affect MITF protein level through the upregulation of MITF gene expression and/or MITF degradation. In the present study, it was proved that MELs inhibits the level of MITF both proteins and transcripts. These data provided the possibilities that MELs may inhibit MITF gene expression via the inactivation of ERK/CREB pathway, rather than MITF degradation.

In summary, the current study herein reports for the first time that MELs could exert anti-melanogenic effects on human melanocytes and human skin equivalent. The current study further reveals that treatment of MELs decreases total cellular tyrosinase activity by decreasing level of tyrosinase expression and suppress melanogenic gene expression through the inhibition of ERK/CREB/MITF signaling pathway. Collectively, my results obtained in the present study could provide an important line of evidence supporting the conclusion that MELs have potential for

development as a potent anti-melanogenic lightening of darkened skin color as well as biosurfactants as a cosmetic ingredient.

CHAPTER II.

MANNOSYLERYTHRITOL LIPIDS AMELIORATE UVA-INDUCED AQUAPORIN-3 DOWNREGULATION BY SUPPRESSING BY c-JUN N-TERMINAL KINASE PHOSPHORYLATION IN CULTURED HUMAN KERATINOCYTES

Abstract

MELs are extracellular glycolipids produced by yeast strains of genus *Pseudozyma*. MELs are commercially used in cosmetics as a biosurfactant, and also reported to show skin-moisturizing efficacy through a yet-unknown underlying mechanism. AQP3 is a membrane protein that contributes to the water homeostasis of the epidermis, and decreased AQP3 expression following UV-irradiation of the skin is associated with reduced skin moisture. No previous study has examined whether the skin-moisturizing effect of MELs might act through the modulation of AQP3 expression. Here, I report for the first time that MELs ameliorate the UVA-induced downregulation of AQP3 in cultured human epidermal keratinocytes (HaCaT cells). My results revealed that UVA irradiation decreases AQP3 expression at the protein and mRNA levels, but that MEL treatment significantly ameliorated these effects. MAPK inhibitor analysis revealed that phosphorylation of c-Jun N-terminal kinase (JNK), but not ERK or p38, mediates UVA-induced AQP3 downregulation, and that MEL treatment significantly suppressed the UVA-induced phosphorylation of JNK. To explore a possible mechanism, I tested whether MELs could regulate the expression of peroxidase proliferator-activated receptor gamma (PPAR-γ), which acts as a potent transcription factor for AQP3 expression. Interestingly, UVA irradiation significantly inhibited the mRNA expression of PPAR-γ in HaCaT cells, whereas a JNK inhibitor and MELs significantly rescued

this effect. Taken together, these findings suggest that MELs ameliorate UVA-induced AQP3 downregulation in human keratinocytes by suppressing JNK activation to block the decrease of PPAR-γ. Collectively, the findings in the current study suggest that MELs can be used as a potential ingredient that modulates AQP3 expression to improve skin moisturization following UVA irradiation-induced damage.

Introduction

MELs are extracellular glycolipids that are produced from different vegetable oil substrates by the yeast strains of genus *Pseudozyma* (Morita, Fukuoka et al. 2015). MELs comprise a hydrophilic headgroup containing 4-O-β-D-mannopyranosyl erythritol or 1-O-β-D-mannopyranosyl erythritol and fatty acid-containing hydrophobic chains (Morita, Fukuoka et al. 2015). MELs were originally developed as a highly biodegradable biosurfactant (Kitamoto, Yanagishita et al. 1993), but were subsequently found to have additional biological properties such as anti-inflammation and apoptosis of melanoma cells (Zhao, Wakamatsu et al. 1999; Wakamatsu, Zhao et al. 2001; Im, Yanagishita et al. 2003; Ueno, Inoh et al. 2007; Morita, Tadokoro et al. 2011). As the possible applications of MELs expanded, some researchers focused on using MELs as a cosmetic ingredient (Morita, Fukuoka et al. 2013); to date, several studies have found that MELs have the potential to affect skin moisturization (Morita, Kitagawa et al. 2009; Yamamoto, Morita et al. 2012).

AQP3 contributes to water homeostasis in the epidermis and is responsible for transporting water and glycerol at the plasma membranes of keratinocytes in the epidermal basal layer (Sugiyama, Ota et al. 2001; Hara, Ma et al. 2002; Hara-Chikuma and Verkman 2005). Decreased AQP3 expression in the skin is associated with dry skin, reduced elasticity, decreased glycerol levels, and impaired wound healing with

defective barrier function (Hara, Ma et al. 2002; Ma, Hara et al. 2002). AQP3 expression in the skin naturally declines with age (Li, Tang et al. 2010), but it may also be reduced by harmful external stimuli, such as UV irradiation and reactive oxygen species (Cao, Wan et al. 2008). Numerous studies have sought to identify materials that may ameliorate the UV irradiation-induced downregulation of AQP3 expression and to evaluate the possible mechanisms underlying such effects (Cao, Wan et al. 2008; Ji, Yang et al. 2010; Shan, Xiao et al. 2012; Jeon, Kang et al. 2015).

The MAPK pathways, namely the ERK, JNK, and p38 pathways, play important roles in regulating and eliciting various cellular responses, such as proliferation, differentiation, development, transformation, and apoptosis (Zhang and Liu 2002). In epidermal keratinocytes, a diverse range of extracellular stimuli, including UV radiation, strongly induce the phosphorylation of MAPKs (Cao, Wan et al. 2008; Ji, Yang et al. 2010; Jeon, Kang et al. 2015). AQP3 expression is reportedly regulated by the MAPK pathways (Cao, Sun et al. 2006; Cao, Wan et al. 2008) as well as by the transcription factor, PPAR-γ, which may be modulated by MAPKs or UV irradiation (Camp, Tafuri et al. 1999; Lee, Lee et al. 2010; Tardelli, Bruschi et al. 2017).

To my knowledge, no previous study had examined whether MELs are involved in modulating AQP3 expression in UV-irradiated keratinocytes. Here, the current study evaluated whether MELs can ameliorate UVA-

induced AQP3 downregulation in cultured human keratinocytes, and then explored a possible underlying mechanism.

Materials and Methods

Reagents

The MELs used in the present study were produced and provided by DKBIO (Daejeon, South Korea). Briefly, MELs were synthesized in a yeast strain of *Pseudozyma* sp., extracted from the culture broth with ethyl acetate, and purified through a fatty acid removal process. Purified MELs were comprised 85% di-acylated MEL-B and 15% tri-acylated MEL, and dissolved with dimethyl sulfoxide for use in the experiments. MAPK inhibitors were purchased from Tocris (#1879, USA) and used at concentrations selected with reference to previous studies (100 nM SP600125 for JNK, 10 μM PD98059 for ERK, and 5 μM SB203580 for p38) (Silvers, Bachelor et al. 2003; Cao, Wan et al. 2008).

Cell culture

HaCaT keratinocytes (an immortalized cell line derived from normal human keratinocytes) were purchased from the American Type Culture Collection (Manassas, VA, USA) and cultured in DMEM (12-604F, Lonza) supplemented with 10% FBS (#10082-147, ThermoFisher Scientific), 100 U/ml potassium penicillin, and 100 mg/ml streptomycin sulfate (17-602E, Lonza) at 37°C in a humidified incubator containing 5% CO_2. The cells were washed with PBS (21-031-CVR, Corning, USA), detached with Accutase™ (SCR005, EMD Millipore, USA), and plated to

60-mm dishes at 0.3 x 10^6 cells/well in fresh culture medium. Cells grown to 70-80% confluence were serum-starved for 4 h and then treated with the indicated concentrations of reagents.

UVA irradiation

UVA irradiation (365 nm) was performed using a microprocessor-controlled, cooled UV irradiation system (Bio-Sun UV-H, VilberLourmat, France). As previously described (Hwang and Shim 2018) cells were covered with serum and phenol red-free DMEM (#21063-029, ThermoFisher Scientific) during irradiation. After irradiation, cells were returned to fresh DMEM (12-604F, Lonza) for culture.

Cell viability assay

Cell viability was determined using a Cell Counting Kit-8 (CCK-8; CK04-05, Dojindo, Japan). HaCaT keratinocytes seeded to a 96-well plate at a density of 5 × 10^3 cells/well were incubated with MELs for 24 h. Then, 10 ㎕ of CCK-8 solution and 90 ㎕ of DMEM (#31053-028, ThermoFisher Scientific) were added to each well and the plate was incubated at 37℃ for 2 h. The absorbance was measured at 450 nm using a microplate reader (Synergy2, BioTek, USA).

RNA extraction and qRT-PCR

Total RNA was extracted using the RNeasy Mini Kit (#74101, Qiagen). One microgram of RNA was reverse transcribed into complementary DNA (cDNA) using a SuperScript® III First-Strand Synthesis System according to the manufacturer's instructions (#18080-051, Invitrogen). For qRT-PCR, we used an ABI 7500 Fast Real-Time PCR system (Applied Biosystems, CA, USA) with the TaqMan™ Gene Expression Master Mix (#4369016, ThermoFisher Scientific) and pre-inventoried TaqMan primers for AQP3 (Hs00185020_m1), PPAR-γ (Hs01115513_m1), and glyceraldehyde-3-phosphate dehydrogenase (GAPDH, detected as a normalization control for cDNA quantity; Hs02786624_g1). The level of relative mRNA expression was calculated using the comparative $\Delta\Delta$Ct method (Livak and Schmittgen 2001).

Western blots analysis

Cells were lysed using RIPA Lysis and Extraction Buffer (#89900, ThermoFisher Scientific) containing a complete mini protease inhibitor (#11836153001, Roche) and a phosphatase inhibitor cocktail (P5726, Sigma). The cell lysates were centrifuged for 20 m at 13,000 rpm and 4°C, and the supernatants were collected for analysis. Protein concentrations were determined using a BCA (bicinchoninic acid) protein assay kit (#23225, ThermoFisher Scientific). Equal amounts of protein (30 μg/well) were loaded to a 4–12% gradient Bis-Tris gel (NP0321PK2,

Nu PAGETM, Invitrogen), separated by SDS-PAGE, and transferred to a nitrocellulose membrane (LC2000, Invitrogen). The membrane was blocked with TBST buffer (0.2% Tween 20 in Tris-buffered saline) containing 5% BSA (A8806, Sigma) at room temperature for 1 h and probed overnight at 4℃ with each of the following primary antibodies: AQP3 (ab125129, Abcam), PPAR-γ (NBP1-61399, Novus), GAPDH (#2118, Cell Signaling Technology), JNK (#9252, Cell Signaling Technology), phospho-JNK (#4668, Cell Signaling Technology), ERK (#4695, Cell Signaling Technology T), phospho-ERK (#4370, Cell Signaling Technology), p38 (#8690, Cell Signaling Technology), and phospho-p38 (#4511, Cell Signaling Technology). After three washes with TBST, the membrane was incubated with horseradish peroxidase-conjugated secondary antibodies at room temperature for 1 h. Chemiluminescent signals were detected with an ECL substrate (RPN2232, GE Healthcare, UK) and visualized using a chemiluminescent detection system (LAS-3000, Fuji Film, Japan).

Statistical analysis

All data are expressed as means ± SD, and the Student's t-test was used for statistical comparisons. A p-value less than 0.05 was considered statistically significant (*, $p < 0.05$; **, $p < 0.01$).

Results

UVA-irradiation downregulates AQP3 expression at the protein and mRNA levels

To determine the optimal dose of UVA for significantly downregulating AQP3 expression in the current experimental system, I irradiated HaCaT keratinocytes with various doses of UVA (0.5, 1, 2, or 3 J/cm^2) and analyzed the protein level of AQP3 after 24 h (Fig 8A). The AQP3 protein level was dose-dependently reduced under UVA irradiation, and significantly decreased to 50% of the level seen in the UVA non-irradiation control group under 3 J/cm^2 of UVA irradiation (UVA 3 J/cm^2) (Fig 8B). Similarly, qRT-PCR revealed that the mRNA expression of AQP3 was significantly reduced to 54% of the control level at 24 h after irradiation with UVA 3 J/cm^2 (Fig 8C). A time-course experiment revealed that a significant decrease in AQP3 mRNA expression could be detected as early as 6 h after UVA irradiation, and this level continued to decrease gradually until 24 h post-irradiation (Fig 8C). Since cell viability was approximately 90% of the control group at 24 h after UVA 3 J/cm^2 irradiation, which was considered not to be significantly different from the control group (Fig 8D), I subsequently used UVA 3 J/cm^2 to significantly reduce AQP3 expression in HaCaT keratinocytes.

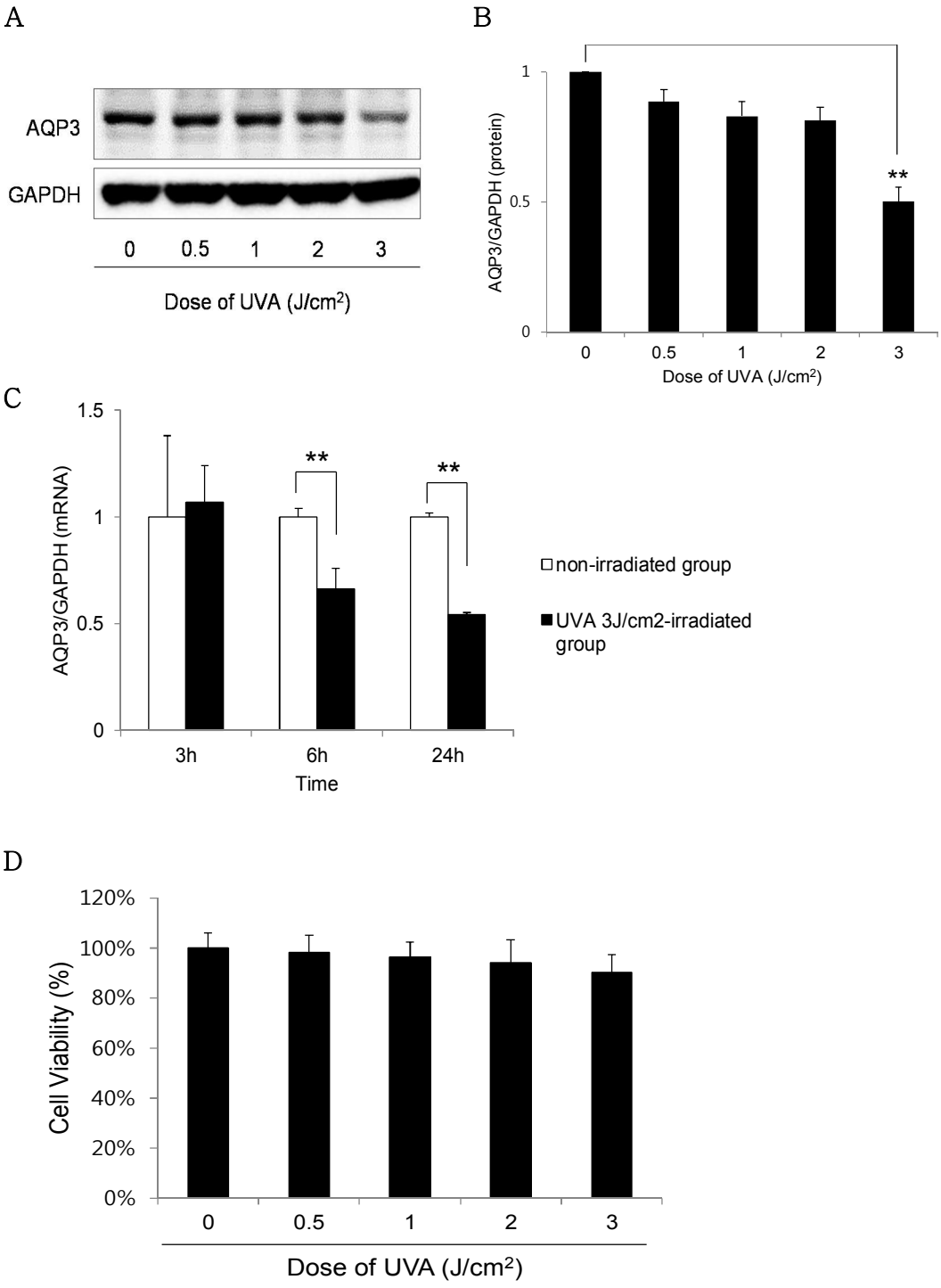
A
AQP3
GAPDH
0
0.5
1
2
3
Dose of UVA (J/cm2)
B
AQP3/GAPDH (protein)
1
0.5
0
**
0
0.5
1
2
3
Dose of UVA (J/cm2)
C
AQP3/GAPDH (mRNA)
1.5
1
0.5
0
**
**
3h
6h
24h
Time
non-irradiated group
UVA 3J/cm2-irradiated group
D
Cell Viability (%)
120%
100%
80%
60%
40%
20%
0%
0
0.5
1
2
3
Dose of UVA (J/cm2)

Fig 8. AQP3 expression is downregulated by UVA irradiation. (A) HaCaT keratinocytes were irradiated with the indicated doses of UVA or left non-irradiated (control) and harvested after 24 h for Western blot analysis. (B) The protein level of AQP3 was quantified relative to that of GAPDH using the NIH ImageJ software. The results are presented as the mean expression level obtained from three independent experiments ± SD (**$p < 0.01$). (C) UVA 3 J/cm^2-irradiated and non-irradiated control cells were harvested at the indicated time points, and qRT-PCR analysis of the AQP3 mRNA level was performed. (D) Effects of UVA-irradiation on the viability of HaCaT keratinocytes. The data were normalized with respect to the expression of GAPDH, and the results are presented as the mean expression ± SD (n=3, ** $p < 0.01$).

MELs ameliorate the UVA-induced downregulation of AQP3

Next, I examined whether MELs could ameliorate the UVA-induced downregulation of AQP3 expression. Non-cytotoxic concentrations of MELs (0.25, 1, and 4 ㎍/ml) were selected based on the results of cell viability assay (Fig 9A) and applied to cells for 24 h following UVA 3 J/cm^2 irradiation. As shown in Fig 9B, the UVA-induced downregulation of AQP3 protein expression was markedly and dose-dependently ameliorated by 1 and 4 ㎍/ml of MELs. These levels were increased by 124% and 142%, respectively, compared to the UVA 3 J/cm^2-irradiated group (Fig 9C). AQP3 mRNA expression was increased by 164% when UVA 3 J/cm^2-irradiated cells were treated with 1 ㎍/ml MELs compared to those receiving UVA 3 J/cm^2 irradiation alone (Fig 9D). This result indicates that MEL 1 ㎍/ml is sufficient to alleviate the UVA-induced reduction of AQP3.

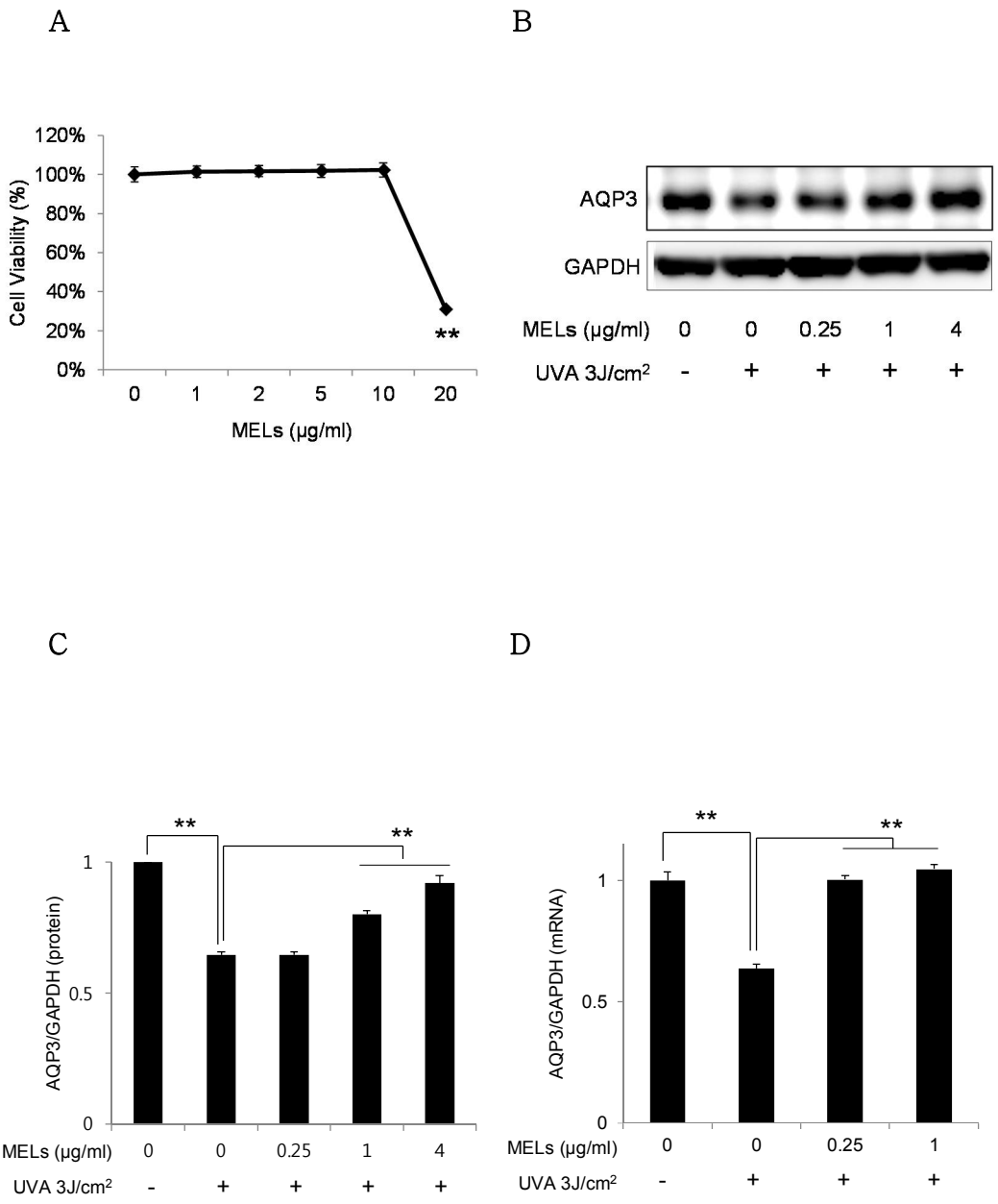
A
B
120%
100%
80%
60%
40%
20%
0%
Cell Viability (%)
**
0
1
2
5
10
20
MELs (μg/ml)
AQP3
GAPDH
MELs (μg/ml) 0 0 0.25 1 4
UVA 3J/cm2 - + + + +
C
D
**
**
1
0.5
0
AQP3/GAPDH (protein)
AQP3/GAPDH (mRNA)
MELs (μg/ml) 0 0 0.25 1 4
UVA 3J/cm2 - + + + +

Fig. 9. MELs ameliorate the UVA-induced downregulation of AQP3 expression in HaCaT keratinocytes. (A) HaCaT keratinocytes were treated with the indicated concentrations of MELs for 24 h and cell viability was determined using a CCK-8 kit. DMSO was used as the vehicle control. (B) Cells treated with UVA 3 J/cm^2 and the indicated concentrations of MELs for 24 h were subjected to Western blot analysis of AQP3 proteins. (C) The protein levels of AQP3 were quantified relative to that of GAPDH using the NIH ImageJ software. (D) The mRNA expression of AQP3 was analyzed by qRT-PCR. The results are presented as the mean expression level obtained from three independent experiments ± SD (**$p < 0.01$).

Phosphorylation of JNK is involved in the UVA-induced downregulation of AQP3

Since the MAPK pathway is reportedly involved in modulating AQP3 expression (Cao, Sun et al. 2006; Cao, Wan et al. 2008), I investigated whether UVA-induced AQP3 downregulation was associated with changes in the MAPKs, JNK, ERK, and p38 MAPK. Serum-starved HaCaT keratinocytes were harvested at 15 m and 30 m after UVA 3 J/cm^2 irradiation. Western blot analyses revealed that the phosphorylation levels of the three MAPKs were significantly increased at both time points compared to those in non-irradiated cells (Fig 10A). Next, I treated serum-starved cells with an inhibitor of each MAPK for 1 h followed by UVA 3 J/cm^2 irradiation, and collected cell lysates 24 h later. I found that the UVA-induced downregulation of AQP3 protein expression was markedly ameliorated by the JNK inhibitor (Fig 10B), which brought this level up to 138% that of the UVA 3 J/cm^2-irradiated group (Fig 10C). Similarly, the mRNA expression level of AQP3 was 136% higher in the JNK inhibitor-treated group than in the UVA 3 J/cm^2-irradiated group (Fig 10D). In contrast, the inhibitors of ERK or p38 failed to rescue the UVA-induced decrease of AQP3 protein expression (Fig 10E).

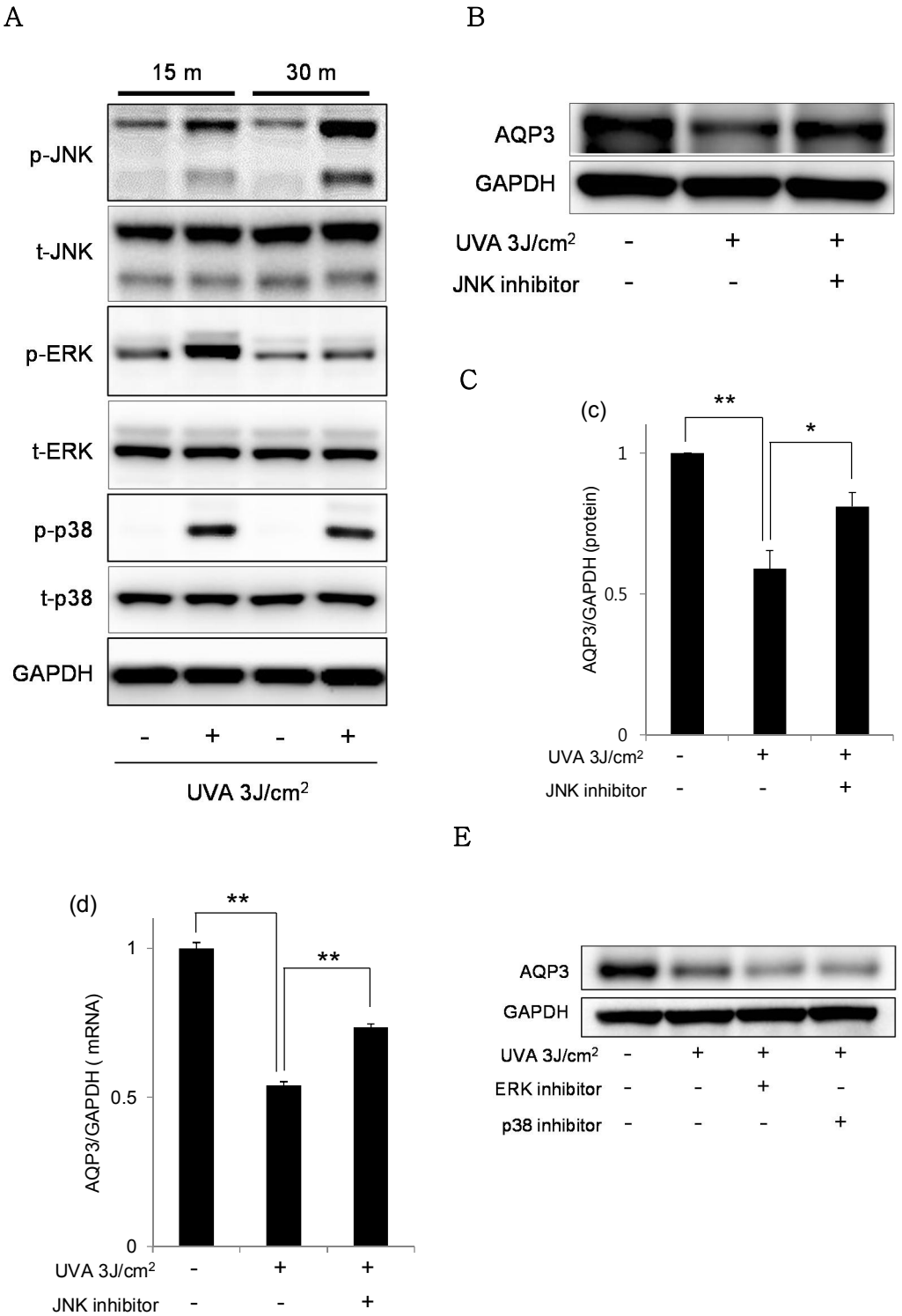
A
15 m
30 m
p-JNK
t-JNK
p-ERK
t-ERK
p-p38
t-p38
GAPDH
- + - +
UVA 3J/cm2
B
AQP3
GAPDH
UVA 3J/cm2 - + +
JNK inhibitor - - +
C
(c)
**
*
AQP3/GAPDH (protein)
1
0.5
0
UVA 3J/cm2 - + +
JNK inhibitor - - +
D
(d)
**
**
AQP3/GAPDH (mRNA)
1
0.5
0
UVA 3J/cm2 - + +
JNK inhibitor - - +
E
AQP3
GAPDH
UVA 3J/cm2 - + + +
ERK inhibitor - - + -
p38 inhibitor - - - +

Fig 10. Involvement of JNK phosphorylation in the UVA-induced downregulation of AQP3. (A) Cells were irradiated with UVA 3 J/cm^2 and harvested at the indicated time points. Protein samples were subjected to Western blotting for phospho-JNK, total JNK, phospho-ERK, total ERK, phospho-p38, total p38, and GAPDH. (B) Cells pretreated with 100 nM SP600125 (a JNK inhibitor) for 1 h were irradiated with UVA 3 J/cm^2 and harvested after 24 h. The protein level of AQP3 was analyzed by Western blotting and (C) quantified relative to the level of GAPDH using the NIH ImageJ software. (D) The mRNA expression of AQP3 was examined by qRT-PCR. (E) Cells pretreated with 10 μM PD98059 (an ERK inhibitor) or 5 μM SB203580 (a p38 inhibitor) for 1 h were irradiated with UVA 3 J/cm^2 and harvested after 24 h. The protein level of AQP3 was evaluated by Western blotting. Values represent the mean expression level $\pm$ SD (n=3, $*p < 0.05$, $**p < 0.01$).

MELs ameliorate UVA-induced AQP3 downregulation by suppressing phosphorylation of JNK

Based on the above findings, I assessed the potential involvement of the MAPK pathway in the ability of MELs to ameliorate the UVA-induced downregulation of AQP3 expression. Serum-starved HaCaT keratinocytes were pretreated with 0.5 or 1 ㎍/ml MELs for 1 h, subjected to UVA 3 J/cm^2 irradiation, and then harvested 15 m later. Indeed, it was found that the UVA-induced upregulation of phosphorylated JNK was suppressed by MEL pretreatment, whereas the levels of phosphorylated ERK and p38 were unchanged (Fig 11A). In an effort to gain further insight into the mechanism through which MELs ameliorate the UVA-induced downregulation of AQP3, we investigated PPAR-γ expression. In line with a previous study (Lee, Lee et al. 2010), it was observed that the mRNA expression of PPAR-γ was downregulated by UVA 3 J/cm^2 irradiation in HaCaT keratinocytes; however, I observed for the first time that this phenomenon was significantly mitigated by MELs or the JNK inhibitor (Fig 11B and 11C).

A

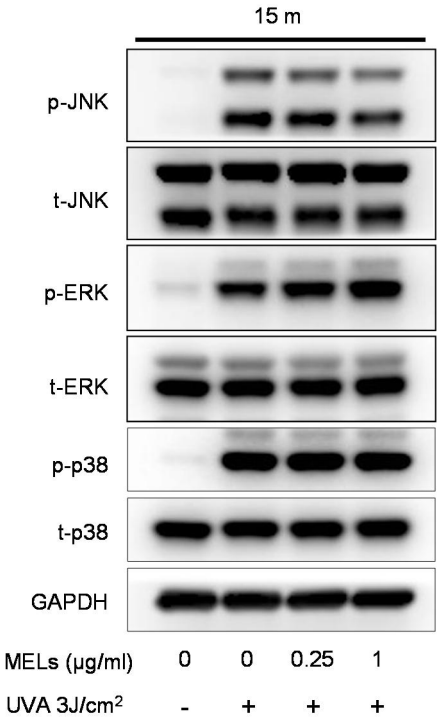
15 m
p-JNK
t-JNK
p-ERK
t-ERK
p-p38
t-p38
GAPDH
MELs (μg/ml) 0 0 0.25 1
UVA 3J/cm2 - + + +

B

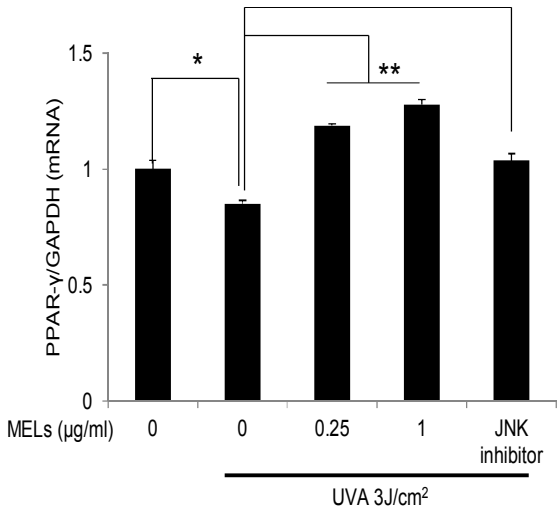
PPAR-γ/GAPDH (mRNA)
1.5
1
0.5
0
*
**
MELs (μg/ml) 0 0 0.25 1 JNK inhibitor
UVA 3J/cm2

C

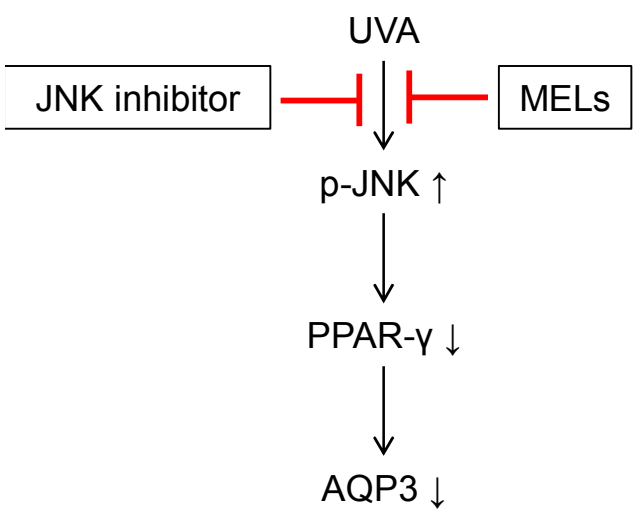
UVA
JNK inhibitor
MELs
p-JNK ↑
PPAR-γ ↓
AQP3 ↓

Fig 11. The effects of MELs on JNK phosphorylation and PPAR-γ expression in UVA-irradiated HaCaT keratinocytes. (A) Cells pretreated with the indicated concentrations of MELs for 1 h were irradiated with UVA 3 J/cm^2 and harvested after 15 m. The protein levels of phospho-JNK, total JNK, phospho-ERK, total ERK, phospho-p38, total p38, and GAPDH were evaluated by Western blot analysis. (B) Cells treated with UVA 3 J/cm^2 and the indicated concentrations of MELs or a JNK inhibitor for 16 h were prepared for qRT-PCR analysis of PPAR-γ mRNA expression. Values represent the mean expression level obtained from three independent experiments ± SD (*$p < 0.05$, **$p < 0.01$). (C) Proposed model showing how MELs ameliorate the UVA-induced downregulation of AQP3.

Discussion

AQP3 is well-known to be involved in skin hydration (Hara-Chikuma and Verkman 2008). Thus, it seems logical that restoring a reduced AQP3 expression level (i.e., that triggered by environmental factors, such as UV irradiation) to its normal level could help improve skin hydration. Numerous studies have sought to identify materials that can effectively ameliorate UVB-induced AQP3 downregulation in HaCaT keratinocytes (Cao, Wan et al. 2008; Ji, Yang et al. 2010; Shan, Xiao et al. 2012; Jeon, Kang et al. 2015). However, UVA irradiation can also induce photo-aging of skin (Kligman 1991) and was reported to reduce AQP3 expression in cultured human keratinocytes (Hwang and Shim 2018). Hwang *et al.* showed that AQP3 mRNA expression was significantly downregulated in UVA 5 J/cm^2-irradiated normal human epidermal keratinocytes, but the authors did not examine any potential underlying mechanism (Hwang and Shim 2018). In the present study, it is confirmed that UVA irradiation markedly reduces AQP3 expression at both the protein and mRNA levels in HaCaT keratinocytes. Furthermore, it is demonstrated that, of the tested MAPK inhibitors, only the JNK inhibitor ameliorates the UVA-induced downregulation of AQP3 in the current experimental system. This suggests that the UVA-activated JNK pathway may be an underlying mechanism through which this irradiation downregulates AQP3. The UVB-induced downregulation of AQP3 expression has been linked with activation of the ERK or p38 pathways

(Cao, Wan et al. 2008; Ji, Yang et al. 2010; Jeon, Kang et al. 2015). These reports found that a JNK inhibitor did little to mitigate the UVB-induced downregulation of AQP3. Although further systematic investigations are warranted, the previous and present findings suggest that the MAPK involved in reducing AQP3 expression in UV-irradiated keratinocytes may differ by the type of UV irradiation.

Various biological effects have been reported for MELs, such as induction of differentiation in mouse melanoma cells and rat pheochromocytoma cells (Zhao, Wakamatsu et al. 1999; Wakamatsu, Zhao et al. 2001), enhancement of plasmid DNA transfection efficiency (Ueno, Inoh et al. 2007), and anti-inflammatory activity (Morita, Tadokoro et al. 2011). Thus, MELs are thought to be versatile candidates for use in various research and industrial fields. In addition, MELs may have potential for cosmetic use in the areas of skin care, damaged hair care, anti-oxidative effects, and facial color make-up (Morita, Kitagawa et al. 2009; Morita, Kitagawa et al. 2010; Takahashi, Morita et al. 2012; Yamamoto, Morita et al. 2012; Morita, Fukuoka et al. 2013). Therefore, it is important to explore their yet-unidentified functions. The present study demonstrates a new biological function of MELs, in that they can alleviate the UVA-induced decrease of AQP3 expression in keratinocytes by suppressing JNK activation. I believe that findings in the current study strengthen the value of MELs as a skin-moisturizing ingredient when combined with its previously reported

efficacies in restoring damaged cells and augmenting water retention in the stratum corneum to hydrate dry skin (Morita, Kitagawa et al. 2009; Yamamoto, Morita et al. 2012). Given that AQP3 expression was found to be downregulated by severe UVA irradiation of normal human skin fibroblasts (Cao, Sun et al. 2006; Xie, Liu et al. 2013), future efforts are warranted to study the effects of MELs against the UVA-induced downregulation of AQP3 in human fibroblasts.

JNK is reportedly involved in regulating PPAR-γ expression. For example, Camp *et al.* found that JNK activation reduced the effect of PPAR-γ ligands by decreasing PPAR-γ mRNA expression (Camp, Tafuri et al. 1999). Meanwhile, Tardelli *et al.* found that activation of the JNK pathway suppressed PPAR-γ to downregulate AQP3 expression in hepatic stellate cells carrying the genetic polymorphism I148M of the patatin-like phospholipase domain-containing 3 (PNPLA3 I148M) (Tardelli, Bruschi et al. 2017). In the abovementioned study, restoration of AQP3 expression was triggered by SP600125-mediated JNK inhibition and/or PPAR-γ stimulation (Tardelli, Bruschi et al. 2017). These findings led me to investigate whether PPAR-γ expression was altered in the current experimental system. Consistent with a previous study showing that PPAR-γ mRNA expression was reduced in UVA-irradiated human adipose tissue-derived mesenchymal stem cells (Lee, Lee et al. 2010), I found that PPAR-γ mRNA expression was downregulated in UVA-irradiated HaCaT keratinocytes. Moreover, this

downregulation of PPAR−γ mRNA expression was markedly counteracted by treatment with a JNK inhibitor or MELs. Based on the present findings, I propose that MELs suppress the UVA-induced phosphorylation of JNK, which prevents the UVA-induced decrease of PPAR−γ expression to ameliorate the reduction of AQP3 expression (Fig 11C).

In summary, the current study herein shows for the first time that MELs can ameliorate UVA-induced AQP3 downregulation in cultured human keratinocytes. It is further revealed that UVA-induced AQP3 downregulation can be ameliorated via the ability of JNK to modulate PPAR−γ expression in cultured human keratinocytes. Collectively, my findings support the potential development of MELs for use in moisturizing skin that has been damaged by UVA irradiation.

GENERAL DISCUSSION AND CONCLUSION

The demonstration of new efficacy for a substance is based on a series of research processes carried out using logical experimental designs and reliable methodologies. First, it is needed to find relevant studies through literature reviews and assess the methods and results shown in those studies. I found the results that a certain type of MELs composed of 54% MEL-A, 25% MEL-B, 14% MEL-C, and 7% MEL-D induce differentiation and apoptosis of mouse B16 melanoma cells and increased melanin content and tyrosinase activity (Zhao, Wakamatsu et al. 1999). Based on these results, I was able to anticipate the potential for MELs to affect melanogenesis and subsequently demonstrated the anti-melanogenic efficacy of current test material MELs (85% di-acylated MEL-B and 15% tri-acylated MEL) using NHMs, mouse B16 melanoma cells, and a three-dimensional human skin equivalent. Moreover, it was also considered important to investigate underlying cellular signaling mechanisms that affect the transcription and protein levels of melanogenic enzymes that directly regulate melanin synthesis to provide a more perspective on the anti-melanogenic efficacy of MELs. As a result, I have confirmed that MELs reduces cellular tyrosinase expression by the ERK/CREB/MITF signaling pathway, thereby suppressing melanogenesis.

The use of reliable experimental methodology in assessing changes in

melanin levels in the melanocytes is one of the most important factors in determining the novel anti-melanogenic effect of test materials. Conventionally, the melanin contents obtained by dissolving the melanocytes treated with the substance are compared with the control cells. Recently, experiments using three-dimensional skin equivalents composed of keratinocytes and melanocytes have been accepted as effective methods to demonstrate the whitening efficacy of test materials (Qiu, Chen et al. 2016; Lee, Lee et al. 2017; Lee, Baek et al. 2018). In order to evaluate the whitening effect on the skin equivalents, the color of the skin equivalent is first measured colorimetrically, and then the special staining for melanin is performed to check whether the color difference is related to the change of melanin synthesis in melanocytes and/or the alteration of melanin transfer to surrounding keratinocytes. Since, however, this method has some limitations in understanding the change and quantification of total melanin contents in three-dimensional skin equivalents, I have adopted a newly developed method of visually and quantitatively evaluating the melanin content. I used two-photon excitation microscopy equipped with a *fs*-pulsed Ti:sapphire laser tuning range of wavelengths from 690 nm to 1050 nm to obtain three-dimensional images and quantify the amounts of melanin distributed throughout the epidermis without processing and sectioning the tissue. I believe that it would be continuously useful in future whitening efficacy studies as a reliable method to measure total melanin contents not only in

melanocytes but also scattered in whole epidermis.

Since melanocytes are located in the basal layer of the epidermis and one melanocyte is reported to be surrounded by 30 to 40 keratinocytes (Fitzpatrick and Breathnach 1963), Topical functional cosmetics or pharmaceuticals containing whitening efficacy are first applied to keratinocytes before melanocytes. Keratinocytes communicate with melanocytes by cell–cell contact as well as secreted factors (Yamaguchi, Brenner et al. 2007). The status of keratinocytes also affects melanin synthesis in nearby melanocytes. Therefore, it was of interest to investigate the effect of MELs, which exert an anti–melanogenic effect on melanocytes in the epidermis, on epidermal keratinocytes. The moisturizing status of the skin is considered as an important factor to look skin brighter, and keratinocytes are reported to play a critical role in skin hydration (Qin, Zheng et al. 2011). Previously reported physical moisturizing effects of MELs on the *in vivo* forearm skin led me to investigate the biological effects associated with moisturizing. I selected AQP3 as a target molecule because it is well–known aquaglyceroporin that transports water and glycerol located in the epidermis. In the present study, I demonstrated that MELs have potential anti–skin dryness effect by exerting ameliorating UVA–irradiation induced AQP3 downregulation. Although many studies have shown a relationship between UVB irradiation and downregulation of AQP3, my study has newly adopted UVA irradiation as a method to reduce AQP3, based on

the rationale that people are more exposed to UVA than UVB in their daily lives. In addition, to my knowledge, I for the first time unraveled underlying mechanism between UVA-irradiation and downregulation of AQP3 in cultured keratinocytes.

Taken together, I have uncovered new efficacies of MELs (85% di-acylated MEL-B and 15% tri-acylated MEL) for skin whitening and moisturizing. This is believed to enhance the value of MELs as functional materials in the cosmetics and pharmaceuticals industry. More importantly, the new experimental methods developed to demonstrate the effectiveness of each will be of great help in further researches involving skin whitening and moisturizing.

국문초록

피부세포와 3 차원 피부 모사체를 이용한 mannosylerythritol lipids 의 미백과 보습효과에 관한 연구

배 일 홍

지도 교수: 김 대 용

서울대학교 대학원 수의학과 수의병리학 전공

Mannosylerythritol lipids (MELs)은 *Pseudozyma* 속의 다양한 효모 균주들 의해 주로 생산되는 세포 외 당지질의 한 종류이다. 현재까지 MELs은 생체 적합성을 띈 바이오 계면 활성제로서 원래의 사용 용도 외에도 몇 가지 생화학적 성질을 가지고 있다고 보고되어 왔다. 또한, MELs을 적용 가능한 산업 분야가 확장됨에 따라 아직 알려지지 않은 MELs의 생물학적 잠재 효능을 발견하기 위한 많은 시도가 이루어지고 있다. 이번 연구에서, 나는 인간 피부 세포 및 3차원 인간 피부 모사체를 사용하여 지금까지 보고되지 않았던 MELs의 피부 미백 및 보습과 관련된 신규 효능과 작용 메커니즘을 입증했다. MELs을 이용한 피부 미백 효능 실험에서 MELs은 정상 인간 멜라닌 형성세포와 알파-멜라닌 형성세포 자극 호르몬을 처리한 B16 마우스 흑색종 세포 모두에서 멜라닌 함량을 유의하게 감소시켰다. 또한 MELs 처리는 멜라닌 형

성세포를 함유한 사람의 인간 피부 모사체에서 색을 밝게 하고 표피의 멜라닌 함량을 감소시키며 미백 효과를 나타내었다. Fontana Masson 염색을 이용한 조직학적 분석에서 멜라닌 형성세포 내 멜라닌 함량은 현저하게 감소된 것으로 관찰되었다. Two-photon excitation microscopy를 사용하여 검출된 멜라닌의 자가 형광 신호 강도는 MELs을 처리한 피부 모사체에서 대조군보다 유의하게 적었다. MELs 처리에 의해 유발된 멜라닌 생성 억제 효과의 근본적인 메카니즘은 타이로시네이즈, 타이로시네이즈 관련 단백질-1 및 타이로시네이즈 관련 단백질-2를 포함하는 필수 멜라닌 생성 효소의 mRNA 발현 수준을 억제하는 ERK/CREB/MITF 신호 전달 경로의 억제와 관련이 있었다. 이어진 MELs의 피부 보습 효능 실험에서, 긴 파장 자외선 조사에 의해 현저히 감소된 aquaporin-3 (AQP3) 발현이 MELs 처리에 의해 인간 각질형성세포주(HaCaT 세포)의 단백질 및 mRNA 수준이 모두 완화되었음을 입증했다. 그리고 MAPK 억제제를 이용하여 JNK 인산화가 긴 파장 자외선에 의한 AQP3 하향 조절에 매개한다는 것과 MELs 처리가 긴 파장 자외선에 의해 유도되는 JNK 인산화를 유의하게 저해한다는 것을 밝혀냈다. 또한 PPAR-γ mRNA 발현이 긴 파장 자외선에 조사 된 HaCaT 세포에서 하향 조절된다는 것을 발견했는데 이러한 현상은 JNK 억제제 또는 MELs의 처리를 통해 현저하게 완화되었다. 이러한 결과는 MELs이 JNK 활성화 억제를 통해 PPAR-γ의 하향조절을 막아 긴 파장 자외선 조사에 의한 AQP3 감소를 완화시킬 수 있다는 것을 제시한다.

상기 결과들을 종합해 볼 때, 나는 이번 일련의 연구들에서 MELs이 멜라닌 형성세포에서 멜라닌 생성과정 억제를 통한 미백 효과와 각질형성세포에서 긴 파장 자외선 조사에 의해 유발되는 AQP3 감소를 억제하는 새로운 효능이

있음을 처음으로 밝혀 보고 하였다. 이를 통해 향후 피부에 안전하고 효과적으로 적용될 수 있는 의약품 또는 화장품에 첨가될 수 있는 기능성 성분으로서의 MELs의 활용 가능성을 기대해 볼 수 있다.

핵심어: mannosylerythritol lipids, 멜라닌 생성, 타이로시네이즈, 피부 모사체, aquaporin-3 (AQP3), 긴 파장 자외선 (자외선 A), c-Jun N-terminal kinase (JNK)

학 번: 2013-30493

REFERENCES

Amiel J., Watkin P. M., Tassabehji M., Read A. P. and Winter R. M. (1998). Mutation of the MITF gene in albinism-deafness syndrome (Tietz syndrome). Clin Dysmorphol 7(1): 17-20.

Andersen W. K., Labadie R. R. and Bhawan J. (1997). Histopathology of solar lentigines of the face: a quantitative study. J Am Acad Dermatol 36(3 Pt 1): 444-447.

Ando H., Kondoh H., Ichihashi M. and Hearing V. J. (2007). Approaches to identify inhibitors of melanin biosynthesis via the quality control of tyrosinase. J Invest Dermatol 127(4): 751-761.

Bonaventure J., Domingues M. J. and Larue L. (2013). Cellular and molecular mechanisms controlling the migration of melanocytes and melanoma cells. Pigment Cell Melanoma Res 26(3): 316-325.

Brenner M. and Hearing V. J. (2008). The protective role of melanin against UV damage in human skin. Photochem Photobiol 84(3): 539-549.

Briganti S., Camera E. and Picardo M. (2003). Chemical and instrumental approaches to treat hyperpigmentation. Pigment Cell Res 16(2): 101-110.

Camp H. S., Tafuri S. R. and Leff T. (1999). c-Jun N-terminal kinase phosphorylates peroxisome proliferator-activated receptor-gamma1 and negatively regulates its transcriptional activity. Endocrinology 140(1): 392-397.

Cao C., Sun Y., Healey S., Bi Z., Hu G., Wan S., Kouttab N., Chu W. and Wan Y. (2006). EGFR-mediated expression of aquaporin-3 is involved in human skin fibroblast migration. Biochem J 400(2): 225-234.

Cao C., Wan S., Jiang Q., Amaral A., Lu S., Hu G., Bi Z., Kouttab N., Chu W. and Wan Y. (2008). All-trans retinoic acid attenuates

ultraviolet radiation-induced down-regulation of aquaporin-3 and water permeability in human keratinocytes. J Cell Physiol 215(2): 506-516.

D'Mello S. A., Finlay G. J., Baguley B. C. and Askarian-Amiri M. E. (2016). Signaling pathways in melanogenesis. Int J Mol Sci 17(7): 1144.

Delijewski M., Wrzesniok D., Beberok A., Rok J., Otreba M. and Buszman E. (2016). The effect of simultaneous exposure of HEMn-DP and HEMn-LP melanocytes to nicotine and UV-radiation on the cell viability and melanogenesis. Environ Res 151: 44-49.

Elias P. M. and Menon G. K. (1991). Structural and lipid biochemical correlates of the epidermal permeability barrier. Adv Lipid Res 24: 1-26.

Fan L., Li H., Niu Y. and Chen Q. (2016). Characterization and inducing melanoma cell apoptosis activity of mannosylerythritol lipids-A Produced from Pseudozyma aphidis. PLoS One 11(2): e0148198.

Fitzpatrick T. B. and Breathnach A. S. (1963). The epidermal melanin unit system. Dermatol Wochenschr 147: 481-489.

Fukuoka T., Morita T., Konishi M., Imura T. and Kitamoto D. (2007). Characterization of new types of mannosylerythritol lipids as biosurfactants produced from soybean oil by a basidiomycetous yeast, Pseudozyma shanxiensis. J Oleo Sci 56(8): 435-442.

Grewal S. S., Fass D. M., Yao H., Ellig C. L., Goodman R. H. and Stork P. J. (2000). Calcium and cAMP signals differentially regulate cAMP-responsive element-binding protein function via a Rap1-extracellular signal-regulated kinase pathway. J Biol Chem 275(44): 34433-34441.

Hara-Chikuma M. and Verkman A. S. (2005). Aquaporin-3 functions as a glycerol transporter in mammalian skin. Biol Cell 97(7): 479-486.

Hara-Chikuma M. and Verkman A. S. (2008). Prevention of skin tumorigenesis and impairment of epidermal cell proliferation by targeted aquaporin-3 gene disruption. Mol Cell Biol 28(1): 326-332.

Hara-Chikuma M. and Verkman A. S. (2008). Roles of aquaporin-3 in the epidermis. J Invest Dermatol 128(9): 2145-2151.

Hara M., Ma T. and Verkman A. S. (2002). Selectively reduced glycerol in skin of aquaporin-3-deficient mice may account for impaired skin hydration, elasticity, and barrier recovery. J Biol Chem 277(48): 46616-46621.

Hara M. and Verkman A. S. (2003). Glycerol replacement corrects defective skin hydration, elasticity, and barrier function in aquaporin-3-deficient mice. Proc Natl Acad Sci U S A 100(12): 7360-7365.

Harding C. R. (2004). The stratum corneum: structure and function in health and disease. Dermatol Ther 17(Suppl 1): 6-15.

Hemesath T. J., Price E. R., Takemoto C., Badalian T. and Fisher D. E. (1998). MAP kinase links the transcription factor Microphthalmia to c-Kit signalling in melanocytes. Nature 391(6664): 298-301.

Ho S. G., Yeung C. K., Chan N. P., Shek S. Y., Kono T. and Chan H. H. (2011). A retrospective analysis of the management of acne post-inflammatory hyperpigmentation using topical treatment, laser treatment, or combination topical and laser treatments in oriental patients. Lasers Surg Med 43(1): 1-7.

Hsiao J. J. and Fisher D. E. (2014). The roles of microphthalmia-associated transcription factor and pigmentation in melanoma. Arch Biochem Biophys 563: 28-34.

Hwang H. S. and Shim J. H. (2018). Brazilin and Caesalpinia sappan L. extract protect epidermal keratinocytes from oxidative stress by inducing the expression of GPX7. Chin J Nat Med 16(3): 203-209.

Im J. H., Nakane T., Yanagishita H., Ikegami T. and Kitamoto D. (2001). Mannosylerythritol lipid, a yeast extracellular glycolipid, shows high binding affinity towards human immunoglobulin G. BMC Biotechnol 1: 5.

Im J. H., Yanagishita H., Ikegami T., Takeyama Y.-i., Idemoto Y., Koura N. and Kitamoto D. (2003). Mannosylerythritol lipids, yeast glycolipid biosurfactants, are potential affinity ligand materials for human immunoglobulin G. J Biomed Mater Res A 65A(3): 379-385.

Imokawa G. and Ishida K. (2014). Inhibitors of intracellular signaling pathways that lead to stimulated epidermal pigmentation: perspective of anti-pigmenting agents. Int J Mol Sci 15(5): 8293-8315.

Inoh Y., Furuno T., Hirashima N., Kitamoto D. and Nakanishi M. (2013). Synergistic effect of a biosurfactant and protamine on gene transfection efficiency. Eur J Pharm Sci 49(1): 1-9.

Isoda H., Kitamoto D., Shinmoto H., Matsumura M. and Nakahara T. (1997). Microbial extracellular glycolipid induction of differentiation and inhibition of the protein kinase C activity of human promyelocytic leukemia cell line HL60. Biosci Biotechnol Biochem 61(4): 609-614.

Jeon B. K., Kang M. K., Lee G. T., Lee K. K., Lee H. S., Woo W. H. and Mun Y. J. (2015). EPA attenuates ultraviolet radiation-induced downregulation of aquaporin-3 in human keratinocytes. Arch Pharm Res 38(8): 1552-1560.

Ji C., Yang Y., Yang B., Xia J., Sun W., Su Z., Yu L., Shan S., He S., Cheng L., Wan Y. and Bi Z. (2010). Trans-Zeatin attenuates ultraviolet induced down-regulation of aquaporin-3 in cultured human skin keratinocytes. Int J Mol Med 26(2): 257-263.

Jimenez-Cervantes C., Martinez-Esparza M., Perez C., Daum N., Solano F. and Garcia-Borron J. C. (2001). Inhibition of melanogenesis in response to oxidative stress: transient downregulation of

melanocyte differentiation markers and possible involvement of microphthalmia transcription factor. J Cell Sci 114(Pt 12): 2335-2344.

Kameyama K., Sakai C., Kuge S., Nishiyama S., Tomita Y., Ito S., Wakamatsu K. and Hearing V. J. (1995). The expression of tyrosinase, tyrosinase-related proteins 1 and 2 (TRP1 and TRP2), the silver protein, and a melanogenic inhibitor in human melanoma cells of differing melanogenic activities. Pigment Cell Res 8(2): 97-104.

Kim D. S., Hwang E. S., Lee J. E., Kim S. Y., Kwon S. B. and Park K. C. (2003). Sphingosine-1-phosphate decreases melanin synthesis via sustained ERK activation and subsequent MITF degradation. J Cell Sci 116(Pt 9): 1699-1706.

Kitamoto D. (2008). Naturally engineered glycolipid biosurfactants leading to distinctive self-assembling properties. Yakugaku Zasshi 128(5): 695-706.

Kitamoto D., Haneishi K., Nakahara T. and Tabuchi T. (1990). Production of mannosylerythritol lipids by Candida antarctica from vegetable oils. Agric Biol Chem 54(1): 37-40.

Kitamoto D., Yanagishita H., Shinbo T., Nakane T., Kamisawa C. and Nakahara T. (1993). Surface active properties and antimicrobial activities of mannosylerythritol lipids as biosurfactants produced by Candida antarctica. J Biotechnol 29(1): 91-96.

Kligman L. H. (1991). The hairless mouse and photoaging. Photochem Photobiol 54(6): 1109-1118.

Kobayashi T., Urabe K., Winder A., Jimenez-Cervantes C., Imokawa G., Brewington T., Solano F., Garcia-Borron J. C. and Hearing V. J. (1994). Tyrosinase related protein 1 (TRP1) functions as a DHICA oxidase in melanin biosynthesis. EMBO J 13(24): 5818-5825.

Konishi M., Maruoka N., Furuta Y., Morita T., Fukuoka T., Imura T. and Kitamoto D. (2014). Biosurfactant-producing yeasts widely inhabit various vegetables and fruits. Biosci Biotechnol Biochem 78(3): 516-523.

Konishi M., Morita T., Fukuoka T., Imura T., Kakugawa K. and Kitamoto D. (2008). Efficient production of mannosylerythritol lipids with high hydrophilicity by Pseudozyma hubeiensis KM-59. Appl Microbiol Biotechnol 78(1): 37-46.

Korner A. and Pawelek J. (1982). Mammalian tyrosinase catalyzes three reactions in the biosynthesis of melanin. Science 217(4565): 1163-1165.

Lee C. S., Baek H. S., Bae I. H., Choi S. J., Kim Y. J., Lee J. H. and Kim J. W. (2018). Depigmentation efficacy of galacturonic acid through tyrosinase regulation in B16 murine melanoma cells and a three-dimensional human skin equivalent. Clin Exp Dermatol 43(6): 708-712.

Lee C. S., Jang W. H., Park M., Jung K., Baek H. S., Joo Y. H., Park Y. H. and Lim K. M. (2013). A novel adamantyl benzylbenzamide derivative, AP736, suppresses melanogenesis through the inhibition of cAMP-PKA-CREB-activated microphthalmia-associated transcription factor and tyrosinase expression. Exp Dermatol 22(11): 762-764.

Lee C. S., Nam G. B. and Park J. S. (2018). Protopanaxatriol inhibits melanin synthesis through inactivation of the pCREB-MITF-tyrosinase signalling pathway in melanocytes. Clin Exp Dermatol 8(10): 13734.

Lee J., Lee J., Jung E., Kim Y.-S., Roh K., Jung K.-H. and Park D. (2010). Ultraviolet A regulates adipogenic differentiation of human adipose tissue-derived mesenchymal stem cells via up-regulation of Kruppel-like factor 2. J Biol Chem 285(42): 32647-32656.

Lee J. H., Lee E. S., Bae I. H., Hwang J. A., Kim S. H., Kim D. Y., Park N. H., Rho H. S., Kim Y. J., Oh S. G. and Lee C. S. (2017).

Antimelanogenic efficacy of melasolv (3,4,5-trimethoxycinnamate thymol ester) in melanocytes and three-dimensional human skin equivalent. Skin Pharmacol Physiol 30(4): 190-196.

Leveque J. L., de Rigal J., Saint-Leger D. and Billy D. (1993). How does sodium lauryl sulfate alter the skin barrier function in man? A multiparametric approach. Skin Pharmacol Physiol 6(2): 111-115.

Levy C., Khaled M. and Fisher D. E. (2006). MITF: master regulator of melanocyte development and melanoma oncogene. Trends Mol Med 12(9): 406-414.

Li J., Tang H., Hu X., Chen M. and Xie H. (2010). Aquaporin-3 gene and protein expression in sun-protected human skin decreases with skin ageing. Australas J Dermatol 51(2): 106-112.

Livak K. J. and Schmittgen T. D. (2001). Analysis of relative gene expression data using real-time quantitative PCR and the 2(-Delta Delta C(T)) Method. Methods 25(4): 402-408.

Ma T., Hara M., Sougrat R., Verbavatz J. M. and Verkman A. S. (2002). Impaired stratum corneum hydration in mice lacking epidermal water channel aquaporin-3. J Biol Chem 277(19): 17147-17153.

Malhotra N. and Dytoc M. (2013). The pathogenesis of vitiligo. J Cutan Med Surg 17(3): 153-172.

Mnif I. and Ghribi D. (2016). Glycolipid biosurfactants: main properties and potential applications in agriculture and food industry. J Sci Food Agric 96(13): 4310-4320.

Morita T., Fukuoka T., Imura T. and Kitamoto D. (2009). Production of glycolipid biosurfactants by basidiomycetous yeasts. Biotechnol Appl Biochem 53(Pt 1): 39-49.

Morita T., Fukuoka T., Imura T. and Kitamoto D. (2013). Production of mannosylerythritol lipids and their application in cosmetics. Appl Microbiol Biotechnol 97(11): 4691-4700.

Morita T., Fukuoka T., Imura T. and Kitamoto D. (2015). Mannosylerythritol lipids: production and applications. J Oleo Sci 64(2): 133-141.

Morita T., Ishibashi Y., Hirose N., Wada K., Takahashi M., Fukuoka T., Imura T., Sakai H., Abe M. and Kitamoto D. (2011). Production and characterization of a glycolipid biosurfactant, mannosylerythritol lipid B, from sugarcane juice by Ustilago scitaminea NBRC 32730. Biosci Biotechnol Biochem 75(7): 1371-1376.

Morita T., Kitagawa M., Suzuki M., Yamamoto S., Sogabe A., Yanagidani S., Imura T., Fukuoka T. and Kitamoto D. (2009). A yeast glycolipid biosurfactant, mannosylerythritol lipid, shows potential moisturizing activity toward cultured human skin cells: the recovery effect of MEL-A on the SDS-damaged human skin cells. J Oleo Sci 58(12): 639-642.

Morita T., Kitagawa M., Yamamoto S., Sogabe A., Imura T., Fukuoka T. and Kitamoto D. (2010). Glycolipid biosurfactants, mannosylerythritol lipids, repair the damaged hair. J Oleo Sci 59(5): 267-272.

Morita T., Konishi M., Fukuoka T., Imura T. and Kitamoto D. (2008). Identification of Ustilago cynodontis as a new producer of glycolipid biosurfactants, mannosylerythritol lipids, based on ribosomal DNA sequences. J Oleo Sci 57(10): 549-556.

Morita T., Konishi M., Fukuoka T., Imura T., Kitamoto H. K. and Kitamoto D. (2007). Characterization of the genus Pseudozyma by the formation of glycolipid biosurfactants, mannosylerythritol lipids. FEMS Yeast Res 7(2): 286-292.

Morita T., Ogura Y., Takashima M., Hirose N., Fukuoka T., Imura T., Kondo Y. and Kitamoto D. (2011). Isolation of Pseudozyma churashimaensis sp. nov., a novel ustilaginomycetous yeast species as a producer of glycolipid biosurfactants, mannosylerythritol lipids. J Biosci Bioeng 112(2): 137-144.

Morita T., Takashima M., Fukuoka T., Konishi M., Imura T. and Kitamoto D. (2010). Isolation of basidiomycetous yeast Pseudozyma tsukubaensis and production of glycolipid biosurfactant, a diastereomer type of mannosylerythritol lipid-B. Appl Microbiol Biotechnol 88(3): 679-688.

Morita Y., Tadokoro S., Sasai M., Kitamoto D. and Hirashima N. (2011). Biosurfactant mannosyl-erythritol lipid inhibits secretion of inflammatory mediators from RBL-2H3 cells. Biochim Biophys Acta 1810(12): 1302-1308.

Pillaiyar T., Namasivayam V., Manickam M. and Jung S. H. (2018). Inhibitors of melanogenesis: an updated review. J Med Chem 61(17): 7395-7418.

Plonka P. M., Handjiski B., Michalczyk D., Popik M. and Paus R. (2006). Oral zinc sulphate causes murine hair hypopigmentation and is a potent inhibitor of eumelanogenesis in vivo. Br J Dermatol 155(1): 39-49.

Qin H., Zheng X., Zhong X., Shetty A. K., Elias P. M. and Bollag W. B. (2011). Aquaporin-3 in keratinocytes and skin: its role and interaction with phospholipase D2. Arch Biochem Biophys 508(2): 138-143.

Qiu J., Chen M., Liu J., Huang X., Chen J., Zhou L., Ma J., Sextius P., Pena A. M., Cai Z. and Jeulin S. (2016). The skin-depigmenting potential of Paeonia lactiflora root extract and paeoniflorin: in vitro evaluation using reconstructed pigmented human epidermis. Int J Cosmet Sci 38(5): 444-451.

Saika A., Koike H., Fukuoka T. and Morita T. (2018). Tailor-made mannosylerythritol lipids: current state and perspectives. Appl Microbiol Biotechnol 102(16): 6877-6884.

Shan S. J., Xiao T., Chen J., Geng S. L., Li C. P., Xu X., Hong Y., Ji C., Guo Y., Wei H., Liu W., Li D. and Chen H. D. (2012). Kanglaite attenuates UVB-induced down-regulation of aquaporin-3 in cultured human skin keratinocytes. Int J Mol Med 29(4): 625-629.

Shibahara S., Takeda K., Yasumoto K., Udono T., Watanabe K., Saito H. and Takahashi K. (2001). Microphthalmia-associated transcription factor (MITF): multiplicity in structure, function, and regulation. J Investig Dermatol Symp Proc 6(1): 99-104.

Silvers A. L., Bachelor M. A. and Bowden G. T. (2003). The role of JNK and p38 MAPK activities in UVA-induced signaling pathways leading to AP-1 activation and c-Fos expression. Neoplasia 5(4): 319-329.

Smith S. D., Kelley P. M., Kenyon J. B. and Hoover D. (2000). Tietz syndrome (hypopigmentation/deafness) caused by mutation of MITF. J Med Genet 37(6): 446-448.

Sugiyama Y., Ota Y., Hara M. and Inoue S. (2001). Osmotic stress up-regulates aquaporin-3 gene expression in cultured human keratinocytes. Biochim Biophys Acta 1522(2): 82-88.

Takahashi M., Morita T., Fukuoka T., Imura T. and Kitamoto D. (2012). Glycolipid biosurfactants, mannosylerythritol lipids, show antioxidant and protective effects against H(2)O(2)-induced oxidative stress in cultured human skin fibroblasts. J Oleo Sci 61(8): 457-464.

Tardelli M., Bruschi F. V., Claudel T., Moreno-Viedma V., Halilbasic E., Marra F., Herac M., Stulnig T. M. and Trauner M. (2017). AQP3 is regulated by PPARγ and JNK in hepatic stellate cells carrying PNPLA3 I148M. Sci Rep 7(1): 14661.

Tsukamoto K., Jackson I. J., Urabe K., Montague P. M. and Hearing V. J. (1992). A second tyrosinase-related protein, TRP-2, is a melanogenic enzyme termed DOPAchrome tautomerase. EMBO J 11(2): 519-526.

Ueno Y., Inoh Y., Furuno T., Hirashima N., Kitamoto D. and Nakanishi M. (2007). NBD-conjugated biosurfactant (MEL-A) shows a new pathway for transfection. J Control Release 123(3): 247-253.

Verkman A. S. (2008). A cautionary note on cosmetics containing ingredients that increase aquaporin-3 expression. Exp Dermatol 17(10): 871-872.

Wakamatsu Y., Zhao X., Jin C., Day N., Shibahara M., Nomura N., Nakahara T., Murata T. and Yokoyama K. K. (2001). Mannosylerythritol lipid induces characteristics of neuronal differentiation in PC12 cells through an ERK-related signal cascade. Eur J Biochem 268(2): 374-383.

Wertz P. W. and van den Bergh B. (1998). The physical, chemical and functional properties of lipids in the skin and other biological barriers. Chem Phys Lipids 91(2): 85-96.

Wu I. B., Lambert C., Lotti T. M., Hercogova J., Sintim-Damoa A. and Schwartz R. A. (2012). Melasma. G Ital Dermatol Venereol 147(4): 413-418.

Wu M., Hemesath T. J., Takemoto C. M., Horstmann M. A., Wells A. G., Price E. R., Fisher D. Z. and Fisher D. E. (2000). c-Kit triggers dual phosphorylations, which couple activation and degradation of the essential melanocyte factor Mi. Genes Dev 14(3): 301-312.

Xie H., Liu F., Liu L., Dan J., Luo Y., Yi Y., Chen X. and Li J. (2013). Protective role of AQP3 in UVA-induced NHSFs apoptosis via Bcl2 up-regulation. Arch Dermatol Res 305(5): 397-406.

Xu W., Gong L., Haddad M. M., Bischof O., Campisi J., Yeh E. T. and Medrano E. E. (2000). Regulation of microphthalmia-associated transcription factor MITF protein levels by association with the ubiquitin-conjugating enzyme hUBC9. Exp Cell Res 255(2): 135-143.

Yamaguchi Y., Brenner M. and Hearing V. J. (2007). The regulation of skin pigmentation. J Biol Chem 282(38): 27557-27561.

Yamamoto S., Morita T., Fukuoka T., Imura T., Yanagidani S., Sogabe A., Kitamoto D. and Kitagawa M. (2012). The moisturizing effects of

glycolipid biosurfactants, mannosylerythritol lipids, on human skin. J Oleo Sci 61(7): 407-412.

Yasumoto K., Yokoyama K., Shibata K., Tomita Y. and Shibahara S. (1995). Microphthalmia-associated transcription factor as a regulator for melanocyte-specific transcription of the human tyrosinase gene. Mol Cell Biol 15(3): 1833.

Yasumoto K., Yokoyama K., Takahashi K., Tomita Y. and Shibahara S. (1997). Functional analysis of microphthalmia-associated transcription factor in pigment cell-specific transcription of the human tyrosinase family genes. J Biol Chem 272(1): 503-509.

Yonei N., Kaminaka C., Kimura A., Furukawa F. and Yamamoto Y. (2012). Two patterns of solar lentigines: a histopathological analysis of 40 Japanese women. J Dermatol 39(10): 829-832.

Yuspa S. H., Dlugosz A. A., Denning M. F. and Glick A. B. (1996). Multistage carcinogenesis in the skin. J Investig Dermatol Symp Proc 1(2): 147-150.

Zhang W. and Liu H. T. (2002). MAPK signal pathways in the regulation of cell proliferation in mammalian cells. Cell Res 12(1): 9-18.

Zhao X., Wakamatsu Y., Shibahara M., Nomura N., Geltinger C., Nakahara T., Murata T. and Yokoyama K. K. (1999). Mannosylerythritol lipid is a potent inducer of apoptosis and differentiation of mouse melanoma cells in culture. Cancer Res 59(2): 482-486.